ADP-12-27/T794
DESY 12-098
Edinburgh 2012/09
LTH 948
June 2012

Scattering phases for meson and baryon resonances on general moving-frame lattices

M. Göckeler[1], R. Horsley[2], M. Lage[3], U.-G. Meißner[3,4], P.E.L. Rakow[5], A. Rusetsky[3], G. Schierholz[6] and J.M. Zanotti[7]

[1] *Institut für Theoretische Physik, Universität Regensburg, 93040 Regensburg, Germany*

[2] *School of Physics and Astronomy, University of Edinburgh, Edinburgh EH9 3JZ, United Kingdom*

[3] *Helmholtz-Institut für Strahlen- und Kernphysik (Theorie) and Bethe Center for Theoretical Physics, Universität Bonn, D-53115 Bonn, Germany*

[4] *Institut für Kernphysik (IKP-3), Institute for Advanced Simulation (IAS-4), Jülich Center for Hadron Physics and JARA – High Performance Computing, Forschungszentrum Jülich, D-52425 Jülich, Germany*

[5] *Theoretical Physics Division, Department of Mathematical Sciences, University of Liverpool, Liverpool L69 3BX, United Kingdom*

[6] *Deutsches Elektronen-Synchrotron DESY, D-22603 Hamburg, Germany*

[7] *CSSM, School of Chemistry and Physics, University of Adelaide, Adelaide SA 5005, Australia*

Abstract

A proposal by Lüscher enables one to compute the scattering phases of elastic two-body systems from the energy levels of the lattice Hamiltonian in a finite volume. In this work we generalize the formalism to S-, P- and D-wave meson and baryon resonances, and general total momenta. Employing nonvanishing momenta has several advantages, among them making a wider range of energy levels accessible on a single lattice volume and shifting the level crossing to smaller values of $m_\pi L$.

PACS numbers: 12.38.Gc

I. INTRODUCTION

Most hadrons are resonances. Lattice simulations of QCD have reached the point now where the masses of up and down quarks are small enough so that the low-lying hadron resonances, such as the $\rho(770)$ and $\Delta(1232)$, can decay via the strong interactions.

Extracting masses and widths of unstable particles from the lattice is made difficult by the fact that resonances cannot be identified directly with a single energy level of the lattice Hamiltonian. Rather, the eigenstates of the lattice Hamiltonian correspond to states that are characteristic of the respective volume. In a series of papers [1] Lüscher has derived the scattering phase shift in the infinite volume from the volume dependence of the energy levels of the lattice Hamiltonian.

The original derivation was given for systems of two identical particles with vanishing total momentum. To compute the scattering phases for a sufficiently large set of energies on a rest-frame lattice, one would have to repeat the calculation on several volumes, which is computationally expensive.

If the total momentum of the resonance is nonzero, however, a wide variety of energy levels are becoming accessible on a single lattice volume, as has been realized by Gottlieb

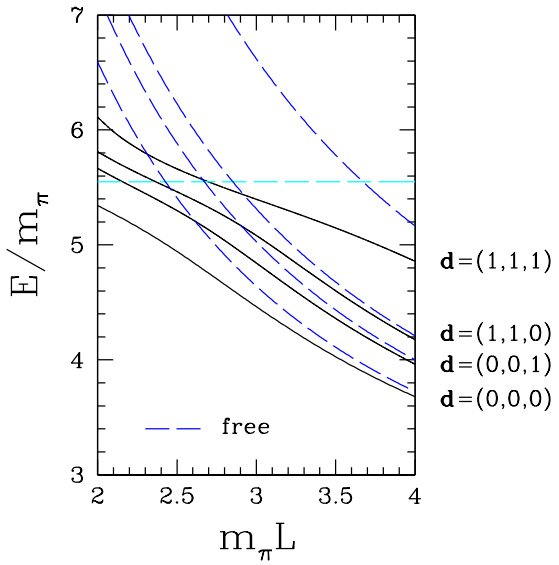

FIG. 1: The ground state CM energy levels of the ρ resonance at the physical point for various momenta $\boldsymbol{P} = (2\pi/L)\,\boldsymbol{d}$, together with the energy levels of the noninteracting $\pi\pi$ system. The horizontal dashed line indicates the physical m_ρ/m_π ratio.

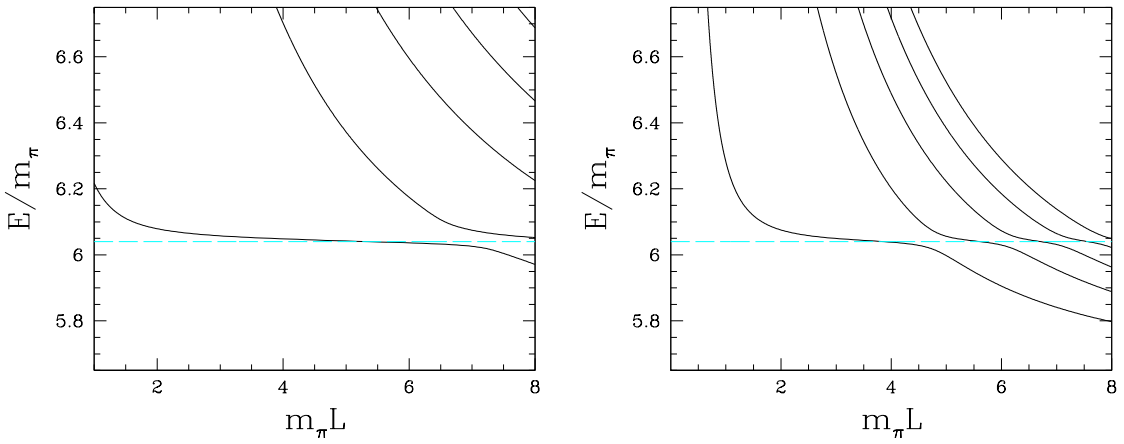

FIG. 2: The expected five lowest CM energy levels of the $\Sigma^*(1385)$ resonance at a pion mass of $m_\pi = 230\,\mathrm{MeV}$ [3] for zero total momentum (left) and $\boldsymbol{P} = 2\pi/L\,\boldsymbol{e}_3$ (right). The dashed line indicates the anticipated m_{Σ^*}/m_π ratio.

and Rummukainen [2]. This is illustrated in Fig. 1, where we show the expected ground state energy level of the ρ resonance for several momenta at the physical pion mass, assuming an effective range approximation for the scattering phase with $g_{\rho\pi\pi} = 6.0$. At a lattice volume of $m_\pi L = 2 \ldots 2.5$ the ground state energy levels of the four lowest momenta are found to cover the resonance region already sufficiently well. Figure 1 tells us, furthermore, that the energy levels of the interacting system rapidly approach the free particle energy spectrum as $m_\pi L$ increases. For zero total momentum this limits the region of practical use to $m_\pi L \lesssim 2.5$, while for nonvanishing total momenta it extends to much larger values of $m_\pi L$.

Of particular interest to us are baryon resonances, which so far have not been explored at all. The low-lying baryon resonances have a much smaller phase space than, for example, the ρ meson, which makes P-wave resonances, such as the Δ and Σ^*, especially hard to tackle. For zero total momentum and $O(200)\,\mathrm{MeV}$ pion masses one would need volumes of $L \approx 6\,\mathrm{fm}$ for the phase shift to cover the region $\delta \approx \pi/2$. The reason is that the pion mass is so much smaller than the mass of the nucleon and the Λ. Not so for nonzero total momenta though, which allows the pion to have zero momentum. In this case the avoided level crossing of the energy levels is shifted towards much smaller values of $m_\pi L$. This is illustrated in Fig. 2, where we compare the expected five lowest energy levels of the Σ^* resonance, that decays to $\Lambda\pi$, for zero and nonzero total momentum, assuming again an effective range approximation

for the scattering phase with $g_{\Sigma^*\Lambda\pi} = 9.2$.

Considering the difficulty of computing the properties of resonances on the lattice, how was ist possible that the mass spectrum of the pseudoscalar and vector meson octet and the baryon decuplet computed in [3, 4], using standard techniques, agreed so well with experiment? The answer is given in Fig. 2. In smaller, favorable volumes the ground state energy may agree well with the resonance mass over a wide range of $m_\pi L$. In larger volumes the ground state energy will approach the energy level of two free particles though.

Gottlieb and Rummukainen have extended Lüscher's work on meson resonances to non-vanishing total momentum $\boldsymbol{P} = (2\pi/L)\,\boldsymbol{e}_3$. Their work was generalized further to two-body systems of arbitrary mass by Davoudi and Savage [5] and Fu [6]. Recently, Feng *et al.* [7] have derived finite size formulae for the next higher momentum $\boldsymbol{P} = (2\pi/L)\,(\boldsymbol{e}_1+\boldsymbol{e}_2)$, which has been generalized again to particles of arbitrary masses by Leskovec and Prelovsek [8]. In the case of unequal masses and nonvanishing momenta the extraction of phase shifts from the energy levels of the lattice Hamiltonian proves difficult, because the partial waves of the individual scattering channels will mix in general. Strategies of how to overcome this problem have been discussed by Döring *et al.* [9] in the framework of unitarized chiral perturbation theory, which is equivalent to Lüscher's approach in the large-L limit. In this work we shall derive phase shift formulae for meson and baryon resonances for total momenta proportional to $\boldsymbol{P} = (2\pi/L)\,\boldsymbol{e}_3$, $\boldsymbol{P} = (2\pi/L)\,(\boldsymbol{e}_1+\boldsymbol{e}_2)$ and $\boldsymbol{P} = (2\pi/L)\,(\boldsymbol{e}_1+\boldsymbol{e}_2+\boldsymbol{e}_3)$, including rotations of $\boldsymbol{P}$. Our formulae will cover all two-body S-, P- and D-wave meson and baryon resonances.

Knowing the scattering phase shifts for general total momenta, among others, we will be able to extract a great variety of other hadronic observables, including elastic and transition form factors of unstable particles, such as the ρ form factor and the Δ to nucleon electromagnetic transition form factors.

The paper is organized as follows. Section II deals with the kinematics of two-particle states on the periodic lattice. In Sec. III we discuss the solutions of the Helmholtz equation for noninteracting and interacting particles. The Lorentz boost from the laboratory frame to the center of mass frame deforms the cubic lattice, and only some subgroups (little groups) of the original cubic point symmetry group remain. In Sec. IV we discuss the symmetry properties of the various center of mass frames, including the representations of the little groups. This is followed by the reduction of the phase shift formulae according to spin,

angular momentum and representation in Sec. V. In Sec. VI we give explicit expressions for the phase shifts of the ρ, Δ and $N^\star(1440)$ (Roper) resonances, and in Sec. VII we give a sample of operators that transform according to some of the prominent representations. Finally, in Sec. VIII we conclude.

II. TWO-PARTICLE KINEMATICS ON A MOVING-FRAME LATTICE

In this section we discuss the kinematical properties of two noninteracting particles of mass m_1 and m_2 in a cubic box of length L with periodic boundary conditions. Twisted boundary conditions will be discussed elsewhere.

Let us first consider the lattice or laboratory (L) frame. We denote the 3-momenta of the individual particles by $\boldsymbol{p}_1, \boldsymbol{p}_2$. The total momentum is denoted by $\boldsymbol{P} = \boldsymbol{p}_1 + \boldsymbol{p}_2$. The energy of two free particles is given by

$$W = \sqrt{\boldsymbol{p}_1^2 + m_1^2} + \sqrt{\boldsymbol{p}_2^2 + m_2^2}\,. \tag{1}$$

The lattice momenta $\boldsymbol{p}_i$ are quantized to

$$\boldsymbol{p}_i = \frac{2\pi}{L}\boldsymbol{n}_i\,, \quad \boldsymbol{n}_i \in \mathbb{Z}^3\,, \tag{2}$$

and, similarly,

$$\boldsymbol{P} = \frac{2\pi}{L}\boldsymbol{d}\,, \quad \boldsymbol{d} \in \mathbb{Z}^3\,. \tag{3}$$

Next, we consider the center-of-mass (CM) frame, which is moving with velocity

$$\boldsymbol{v} = \frac{\boldsymbol{P}}{W}\,, \quad v = |\boldsymbol{v}| \tag{4}$$

in the laboratory frame. We denote the CM (relative) momentum by $\boldsymbol{k}$ and the energy by E. Momentum and energy are obtained by a standard Lorentz transformation,

$$\boldsymbol{k} = \boldsymbol{\gamma}\left(\boldsymbol{p}_1 - \boldsymbol{v}\sqrt{\boldsymbol{p}_1^2 + m_1^2}\right) = -\boldsymbol{\gamma}\left(\boldsymbol{p}_2 - \boldsymbol{v}\sqrt{\boldsymbol{p}_2^2 + m_2^2}\right)\,, \tag{5}$$

where

$$\boldsymbol{\gamma p} = \gamma \boldsymbol{p}_\parallel + \boldsymbol{p}_\perp\,, \quad \gamma = \frac{1}{\sqrt{1-v^2}} = \frac{W}{E} \tag{6}$$

and

$$\boldsymbol{p}_\parallel = \boldsymbol{v}\,\frac{\boldsymbol{vp}}{v^2}\,, \quad \boldsymbol{p}_\perp = \boldsymbol{p} - \boldsymbol{p}_\parallel\,. \tag{7}$$

Laboratory and CM frame energies are related by

$$W = \sqrt{\boldsymbol{P}^2 + E^2}\,, \tag{8}$$

where

$$E = E_1 + E_2 = \sqrt{\boldsymbol{k}^2 + m_1^2} + \sqrt{\boldsymbol{k}^2 + m_2^2}\,, \quad \boldsymbol{k}^2 = \frac{\left(E^2 - (m_1^2 + m_2^2)\right)^2 - 4m_1^2 m_2^2}{4E^2}\,. \tag{9}$$

Defining

$$\boldsymbol{p} = \frac{1}{2}\,(\boldsymbol{p}_1 - \boldsymbol{p}_2) = \boldsymbol{p}_1 - \frac{1}{2}\,\boldsymbol{P} = -\boldsymbol{p}_2 + \frac{1}{2}\,\boldsymbol{P}\,, \tag{10}$$

and expressing the laboratory frame energies in (5) by their CM counterparts, the CM momentum $\boldsymbol{k}$ can be rewritten as

$$\boldsymbol{k} = \boldsymbol{\gamma}^{-1}\boldsymbol{p} - \gamma^{-1}\,\frac{m_1^2 - m_2^2}{E^2}\,\frac{1}{2}\,\boldsymbol{P}\,, \quad \boldsymbol{\gamma}^{-1}\boldsymbol{p} = \gamma^{-1}\boldsymbol{p}_\parallel + \boldsymbol{p}_\perp\,. \tag{11}$$

This results in the quantization condition

$$\boldsymbol{k} \in \mathit{\Gamma}_{\boldsymbol{\Delta}} \tag{12}$$

with

$$\mathit{\Gamma}_{\boldsymbol{\Delta}} = \left\{ \boldsymbol{k} \,\middle|\, \boldsymbol{k} = \frac{2\pi}{L}\boldsymbol{\gamma}^{-1}\left(\boldsymbol{n} - \frac{1}{2}\,\boldsymbol{\Delta}\right),\, \boldsymbol{n} \in \mathbb{Z}^3 \right\}, \quad \boldsymbol{\Delta} = \boldsymbol{d}\left(1 + \frac{m_1^2 - m_2^2}{E^2}\right). \tag{13}$$

III. SOLUTIONS OF THE HELMHOLTZ EQUATION

To compute the scattering phases of the interacting two-particle system, we need to discuss the solutions of the Helmholtz equation [10] in the CM frame first.

In the laboratory frame the two-particle state is described by the wave function $\psi_L(x_1; x_2)$, where $x_1 = (x_1^0, \boldsymbol{x}_1)$, $x_2 = (x_2^0, \boldsymbol{x}_2)$ are the space-time coordinates in Minkowski space. For the moment we restrict ourselves to particles of spin zero. The wave function can then be written

$$\psi_L(x_1; x_2) = e^{-i(Wt - \boldsymbol{P}\boldsymbol{X})}\,\phi_L(x_0, \boldsymbol{x}) \tag{14}$$

with

$$\begin{aligned} \boldsymbol{X} &= \frac{m_1\boldsymbol{x}_1 + m_2\boldsymbol{x}_2}{m_1 + m_2}\,, \quad \boldsymbol{x} = \boldsymbol{x}_1 - \boldsymbol{x}_2\,, \\ t &= \frac{m_1 x_1^0 + m_2 x_2^0}{m_1 + m_2}\,, \quad x^0 = x_1^0 - x_2^0\,. \end{aligned} \tag{15}$$

We are interested in the case where both particles have equal time coordinates, $x_1^0 = x_2^0 = t$.

We denote the space-time separation in the CM frame by $r = (r^0, \boldsymbol{r})$. The transformation from the laboratory frame to the CM is given by

$$\begin{pmatrix} r^0 \\ \boldsymbol{r} \end{pmatrix} = \begin{pmatrix} \gamma & \gamma\,\boldsymbol{v} \\ \boldsymbol{\gamma}\boldsymbol{v} & \boldsymbol{\gamma} \end{pmatrix} \begin{pmatrix} 0 \\ \boldsymbol{x} \end{pmatrix} \tag{16}$$

with

$$\phi_L(0,\boldsymbol{x}) = \phi_{CM}(r^0,\boldsymbol{r})\,. \tag{17}$$

In the case of unequal masses, $m_1 \neq m_2$, the (relative) time coordinate r^0 is no longer zero, even though x^0 is.

A. Noninteracting particles

For noninteracting particles the CM frame wave function obeys the equation of motion

$$\left(-\nabla_{r^0}^2 + \boldsymbol{\nabla}_{\boldsymbol{r}}^2 + \left(E^2 - (m_1+m_2)^2\right)\frac{m_1 m_2}{(m_1+m_2)^2}\right)\,\phi_{CM}(r^0,\boldsymbol{r}) = 0 \tag{18}$$

with

$$\left(-i\,\nabla_{r^0} - \frac{E_1 m_2 - E_2 m_1}{m_1+m_2}\right)\,\phi_{CM}(r^0,\boldsymbol{r}) = 0\,. \tag{19}$$

Equations (18) and (19) follow directly from the Klein-Gordon equations of the individual particles. Writing

$$\phi_{CM}(r^0,\boldsymbol{r}) = e^{i\,\frac{E_1 m_2 - E_2 m_1}{m_1+m_2}\,r^0}\,\phi_{CM}(0,\boldsymbol{r})\,, \tag{20}$$

the time dependence can be factored out, and we obtain the Helmholtz equation

$$\left(\boldsymbol{\nabla}_{\boldsymbol{r}}^2 + \boldsymbol{k}^2\right)\,\phi_{CM}(\boldsymbol{r}) = 0 \tag{21}$$

with $\phi_{CM}(\boldsymbol{r}) = \phi_{CM}(0,\boldsymbol{r})$, and $\boldsymbol{k}$ given by (13).

The laboratory frame wave function is periodic under spatial translations

$$\psi_L(x_1^0,\boldsymbol{x}_1;x_2^0,\boldsymbol{x}_2) = \psi_L(x_1^0,\boldsymbol{x}_1+\boldsymbol{n}_1 L;x_2^0,\boldsymbol{x}_2+\boldsymbol{n}_2 L)\,,\quad \boldsymbol{n}_{1,2}\in\mathbb{Z}^3. \tag{22}$$

Equations (14), (17) and (20) together give

$$\psi_L(0,\boldsymbol{x}_1;0,\boldsymbol{x}_2) = e^{i\left(\boldsymbol{P}\boldsymbol{X}+\frac{E_1 m_2 - E_2 m_1}{E(m_1+m_2)}\boldsymbol{P}\boldsymbol{x}\right)}\,\phi_{CM}(\boldsymbol{r})\,, \tag{23}$$

where we have inserted $r^0 = \gamma\,\boldsymbol{v}\boldsymbol{x} = \boldsymbol{P}\boldsymbol{x}/E$. This leads to the periodicity relation for the CM wave function

$$\phi_{CM}(\boldsymbol{r}) = e^{-i\,\pi\,\boldsymbol{n}\boldsymbol{\Delta}}\,\phi_{CM}(\boldsymbol{r}+\boldsymbol{\gamma}\boldsymbol{n}L) \tag{24}$$

with $\boldsymbol{n} = \boldsymbol{n}_1 - \boldsymbol{n}_2$. While for equal masses $\phi_{CM}(\boldsymbol{r})$ is either periodic ($\boldsymbol{n}$ even) or antiperiodic ($\boldsymbol{n}$ odd) with period γL, this is no longer so for $m_1 \neq m_2$. In this case the CM wave function picks up a complex phase factor $e^{-i\,\pi\,\boldsymbol{n}\boldsymbol{\Delta}}$ when crossing the spatial boundary. We call this attribute $\boldsymbol{\Delta}$-periodic.

B. Interacting particles

Let us now turn to the interacting case. We assume that the two-body interaction has finite range and vanishes outside the region $|\boldsymbol{r}| > R$ with $L \gg 2R$. In the exterior region $\phi_{CM}(\boldsymbol{r})$ satisfies the Helmholtz equation

$$\left(\boldsymbol{\nabla}_{\boldsymbol{r}}^2 + \boldsymbol{k}^2\right)\, \phi_{CM}(\boldsymbol{r}) = 0 \tag{25}$$

with

$$\boldsymbol{k}^2 = \frac{\left(E^2 - (m_1^2 + m_2^2)\right)^2 - 4m_1^2 m_2^2}{4E^2} \equiv k^2\,, \tag{26}$$

where E now are the energy levels of the interacting system.

We are now looking for solutions of the Helmholtz equation (25). The (singular) case $\boldsymbol{k} \in \Gamma_{\boldsymbol{\Delta}}$ requires a separate discussion, which we shall omit here. The Green function

$$G^{\boldsymbol{\Delta}}(\boldsymbol{r}, k^2) = \gamma^{-1} L^{-3} \sum_{\boldsymbol{p} \in \Gamma_{\boldsymbol{\Delta}}} \frac{e^{\,i\,\boldsymbol{p}\boldsymbol{r}}}{\boldsymbol{p}^2 - k^2} \tag{27}$$

is such a solution. An appropriate basis of solutions of the Helmholtz equation is obtained from (27) by

$$G^{\boldsymbol{\Delta}}_{lm}(\boldsymbol{r}, k^2) = \mathcal{Y}_{lm}(\boldsymbol{\nabla})\, G^{\boldsymbol{\Delta}}(\boldsymbol{r}, k^2)\,, \tag{28}$$

where

$$\mathcal{Y}_{lm}(\boldsymbol{r}) = |\boldsymbol{r}|^l\, Y_{lm}(\hat{\boldsymbol{r}})\,, \quad \hat{\boldsymbol{r}} = \frac{\boldsymbol{r}}{|\boldsymbol{r}|}\,. \tag{29}$$

Obviously, $G^{\boldsymbol{\Delta}}(\boldsymbol{r}, k^2)$ and $G^{\boldsymbol{\Delta}}_{lm}(\boldsymbol{r}, k^2)$ are $\boldsymbol{\Delta}$-periodic. The CM wave function can then be expanded as

$$\phi_{CM}(\boldsymbol{r}) = \sum_{l,m} c_{lm}\, G^{\boldsymbol{\Delta}}_{lm}(\boldsymbol{r}, k^2)\,, \tag{30}$$

which may be interpreted as a partial wave expansion. The functions $G^{\boldsymbol{\Delta}}_{lm}$ can be expanded in spherical harmonics $Y_{lm}(\theta, \varphi)$ and spherical Bessel functions [11] $n_l(kr)$, $j_l(kr)$

$$G^{\boldsymbol{\Delta}}_{lm}(\boldsymbol{r}, k^2) = \frac{(-1)^l\, k^{l+1}}{4\pi} \left[n_l(kr)\, Y_{lm}(\theta, \varphi) + \sum_{l'=0}^{\infty} \sum_{m'=-l'}^{l'} M^{\boldsymbol{\Delta}}_{lm,l'm'}\, j_{l'}(kr)\, Y_{l'm'}(\theta, \varphi) \right] \tag{31}$$

with

$$M^{\boldsymbol{\Delta}}_{lm,l'm'} = \frac{(-1)^l\, \gamma^{-1}}{\pi^{3/2}} \sum_{j=|l-l'|}^{l+l'} \sum_{s=-j}^{j} \frac{i^j}{q^{j+1}}\, Z^{\boldsymbol{\Delta}}_{js}(1, q^2)^*\, C_{lm,js,l'm'}\,, \quad q = \frac{kL}{2\pi}\,, \tag{32}$$

where $r = |\boldsymbol{r}|, \theta$ and φ are the polar coordinates of $\boldsymbol{r}$. The generalized zeta function $Z_{js}^{\boldsymbol{\Delta}}(1, q^2)$ is obtained from

$$Z_{js}^{\boldsymbol{\Delta}}(\delta, q^2) = \sum_{\boldsymbol{z} \in P_{\boldsymbol{\Delta}}} \frac{\mathcal{Y}_{js}(\boldsymbol{z})}{(\boldsymbol{z}^2 - q^2)^{\delta}} \tag{33}$$

with

$$P_{\boldsymbol{\Delta}} = \left\{ \boldsymbol{z} \,\middle|\, \boldsymbol{z} = \boldsymbol{\gamma}^{-1} \left(\boldsymbol{n} - \frac{1}{2}\,\boldsymbol{\Delta} \right) ,\, \boldsymbol{n} \in \mathbb{Z}^3 \right\} \tag{34}$$

by analytic continuation $\delta \to 1$. The coefficient $C_{lm,js,l'm'}$ can be expressed in terms of Wigner $3j$-symbols

$$C_{lm,js,l'm'} = (-1)^{m'}\, i^{l-j+l'} \sqrt{(2l+1)(2j+1)(2l'+1)} \begin{pmatrix} l & j & l' \\ m & s & -m' \end{pmatrix} \begin{pmatrix} l & j & l' \\ 0 & 0 & 0 \end{pmatrix} . \tag{35}$$

In Appendix A we give $Z_{js}^{\boldsymbol{\Delta}}(1, q^2)$ for arbitrary values of j and s.

It is easily seen that

$$\begin{aligned} &\left\{ \boldsymbol{z} \,\middle|\, \boldsymbol{z} = \boldsymbol{\gamma}^{-1} \left(\boldsymbol{n} - \frac{1}{2}\,\boldsymbol{\Delta}(m_1, m_2) \right) ,\, \boldsymbol{n} \in \mathbb{Z}^3 \right\} \\ &= \left\{ -\boldsymbol{z} \,\middle|\, \boldsymbol{z} = \boldsymbol{\gamma}^{-1} \left(\boldsymbol{n} - \frac{1}{2}\,\boldsymbol{\Delta}(m_2, m_1) \right) ,\, \boldsymbol{n} \in \mathbb{Z}^3 \right\} . \end{aligned} \tag{36}$$

This results in

$$Z_{js}^{\boldsymbol{\Delta}(m_1,m_2)}(\delta, q^2) = (-1)^j\, Z_{js}^{\boldsymbol{\Delta}(m_2,m_1)}(\delta, q^2) \tag{37}$$

and

$$M_{lm,l'm'}^{\boldsymbol{\Delta}(m_1,m_2)} = (-1)^{l+l'}\, M_{lm,l'm'}^{\boldsymbol{\Delta}(m_2,m_1)} , \tag{38}$$

as $l + j + l' =$ even. Both $M_{lm,l'm'}^{\boldsymbol{\Delta}(m_1,m_2)}$ and $M_{lm,l'm'}^{\boldsymbol{\Delta}(m_2,m_1)}$ have the same determinant and lead to the same results, so that the order of m_1 and m_2 does not matter.

In the literature one often finds the expression [2, 8]

$$M_{lm,l'm'}^{\boldsymbol{\Delta}} = \frac{(-1)^l\, \gamma^{-1}}{\pi^{3/2}} \sum_{j=|l-l'|}^{l+l'} \sum_{s=-j}^{j} \frac{i^j}{q^{j+1}}\, Z_{js}^{\boldsymbol{\Delta}}(1, q^2)\, C_{lm,js,l'm'} . \tag{39}$$

Though not quite correct in general, it leads to the same results for the phase shifts as the matrix (32). Indeed, if we denote (39) by $\tilde{M}$, we find $\tilde{M}_{lm,l'm'} = (-1)^{l+l'}\, M_{lm,l'm'}^{*}$, which has the same determinant as M (see the equations for the phase shifts given in (54) and (55) below). In the following we shall use the short-hand notation

$$w_{lm} = \frac{1}{\pi^{3/2}\sqrt{2l+1}} \gamma^{-1} q^{-l-1}\, Z_{lm}^{\boldsymbol{\Delta}}(1, q^2) . \tag{40}$$

So far we have considered spinless particles only. Let us now assume that one of the particles carries spin S. In the outer region $|\boldsymbol{r}| > R$, which we are concerned with here, the spin operator $\hat{S}$ commutes with the Hamiltonian. The spin-dependent part of the wave function can thus be factored out. As we are mainly interested in meson-baryon resonances, we consider $S = 1/2$. In this case we have

$$\phi_{CM}(\boldsymbol{r}) = \sum_{\substack{J,\mu \\ l,m,\sigma}} \langle lm, \frac{1}{2}\sigma | J\mu \rangle \, c_{lm} \, G^{\boldsymbol{\Delta}}_{lm}(\boldsymbol{r}, q^2) \, \chi^{\frac{1}{2}}_{\sigma} \,, \tag{41}$$

where $\chi^{\frac{1}{2}}_{\sigma}$ is the two-component baryon spinor. This amounts to an expansion of the CM wave function in terms of spin sperical harmonics

$$Y_{Jl\mu} = \sum_{m,\sigma} \langle lm, \frac{1}{2}\sigma | J\mu \rangle \, Y_{lm} \, \chi^{\frac{1}{2}}_{\sigma} \,. \tag{42}$$

In this basis the matrix $M^{\boldsymbol{\Delta}}$ reads

$$M^{\boldsymbol{\Delta}}_{Jl\mu,J'l'\mu'} = \sum_{\substack{m,\sigma \\ m',\sigma'}} \langle lm, \frac{1}{2}\sigma | J\mu \rangle \, \langle l'm', \frac{1}{2}\sigma' | J'\mu' \rangle \, M^{\boldsymbol{\Delta}}_{lm,l'm'} \,. \tag{43}$$

IV. SYMMETRY PROPERTIES

The Lorentz boost deforms the cubic box to a parellelepiped, in which the length scale parallel to the direction of the boost vector is multiplied by γ, whereas the perpendicular length scale is left unchanged.

A. Boost vectors

We will consider boost vectors

$$\boldsymbol{d} = (d_1, d_2, d_3) \,, \quad d_i = 0, \pm 1 \tag{44}$$

and integer multiples $n\,\boldsymbol{d}$, $n \in \mathbb{Z}$ thereof. For that purpose it is sufficient to consider

$$\begin{aligned} \boldsymbol{d} = (0,0,0) \equiv \boldsymbol{0} \quad &, \quad \boldsymbol{d} = (0,0,1) \equiv \boldsymbol{e}_3 \,, \\ \boldsymbol{d} = (1,1,0) \equiv \boldsymbol{e}_1 + \boldsymbol{e}_2 \quad &, \quad \boldsymbol{d} = (1,1,1) \equiv \boldsymbol{e}_1 + \boldsymbol{e}_2 + \boldsymbol{e}_3 \,. \end{aligned} \tag{45}$$

The boost vectors (44) can be transformed into one of the boost vectors (45) by a global rotation, which will leave our final results unchanged. Results for multiples of (45) are

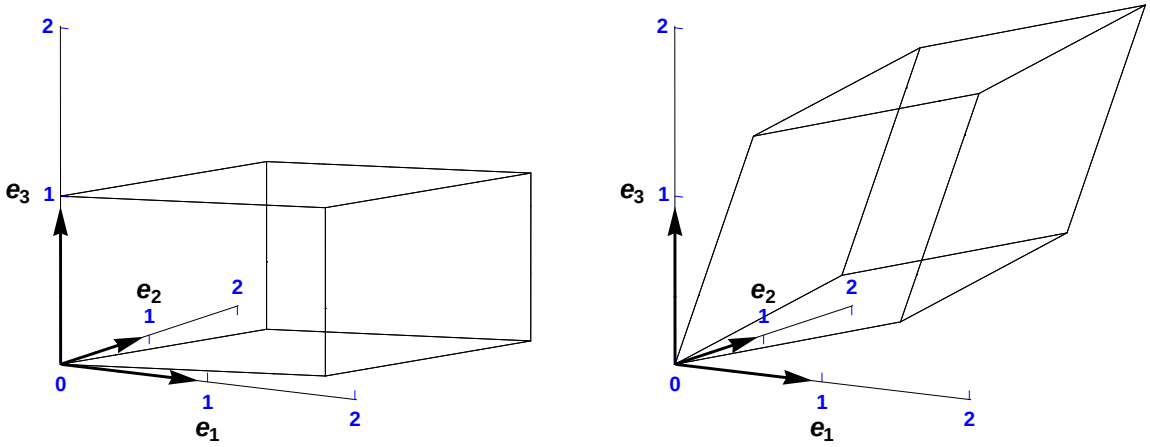

FIG. 3: A cubic box of unit length deformed to a parallelepiped with $\boldsymbol{d} = (\boldsymbol{e}_1 + \boldsymbol{e}_2)$ (left panel) and $\boldsymbol{d} = (\boldsymbol{e}_1 + \boldsymbol{e}_2 + \boldsymbol{e}_3)$ (right panel) for $\gamma = 2$.

obtained by simply replacing $\boldsymbol{d}$ by $n\,\boldsymbol{d}$ in the formulae to follow. In Fig. 3 we show two examples of the deformation of the cubic box.

B. Properties of the functions w_{lm}

In the following we shall use the shorthand notation

$$\boldsymbol{w}_l = (w_{ll}, w_{ll-1}, \cdots w_{l\,-l+1}, w_{l\,-l})\,. \tag{46}$$

As a result of (37), w_{lm} is no longer zero for odd values of l in the case of unequal masses. In general we have

$$Z^{\boldsymbol{\Delta}}_{l-m}(1;q^2) = (-1)^m Z^{\boldsymbol{\Delta}}_{lm}(1;q^2)^*\,. \tag{47}$$

1. *The case* $\boldsymbol{d} = (0,0,1)$

In this case the system is symmetric under rotations around $\boldsymbol{e}_3$ by $\pi/2$, which leads to

$$Z^{\boldsymbol{\Delta}}_{lm}(1;q^2) = 0\,, \quad \text{for } m \neq 0 \mod 4\,. \tag{48}$$

Furthermore, the system is symmetric under the interchange of axes $1 \leftrightarrow 2$, as well as reflections $\boldsymbol{e}_{1,2} \to -\boldsymbol{e}_{1,2}$. This leaves us with the following elements

l	$\boldsymbol{w}_l$
0	(w_{00})
1	$(0, w_{10}, 0)$
2	$(0, 0, w_{20}, 0, 0)$
3	$(0, 0, 0, w_{30}, 0, 0, 0)$
4	$(w_{44}, 0, 0, 0, w_{40}, 0, 0, 0, w_{44})$

2. The case $\boldsymbol{d} = (1, 1, 0)$

In this case the system is symmetric under the interchange of the axes $1 \leftrightarrow 2$. Furthermore, the system is symmetric under reflections $\boldsymbol{e}_3 \to -\boldsymbol{e}_3$. This leaves us with the following elements

l	$\boldsymbol{w}_l$
0	(w_{00})
1	$\sqrt{2}\,\mathrm{Re}\, w_{11}\ \left(e^{i\pi/4}, 0, -e^{-i\pi/4}\right)$
2	$(w_{22}, 0, w_{20}, 0, -w_{22})$
3	$\sqrt{2}\ \left(e^{-i\pi/4}\mathrm{Re}\, w_{33}, 0, e^{i\pi/4}\mathrm{Re}\, w_{31}, 0, -e^{-i\pi/4}\mathrm{Re}\, w_{31}, 0, -e^{i\pi/4}\mathrm{Re}\, w_{33}\right)$
4	$(w_{44}, 0, w_{42}, 0, w_{40}, 0, -w_{42}, 0, w_{44})$

3. The case $\boldsymbol{d} = (1, 1, 1)$

In this case the only symmetry that is left is the symmetry under cyclic permutation $1 \to 2 \to 3 \to 1$. This leaves us with the following elements

l	$\boldsymbol{w}_l$
0	(w_{00})
1	$w_{10}\ \left(-e^{i\pi/4}, 1, e^{-i\pi/4}\right)$
2	$w_{22}\ \left(1, -\sqrt{2}e^{-i\pi/4}, 0, -\sqrt{2}e^{i\pi/4}, -1\right)$
3	$\left(-\frac{\sqrt{10}}{4}\, e^{-i\pi/4}w_{30}, w_{32}, \frac{\sqrt{6}}{4}\, e^{i\pi/4}\, w_{30}, w_{30}, -\frac{\sqrt{6}}{4}\, e^{-i\pi/4}\, w_{30}, -w_{32}, \frac{\sqrt{10}}{4}\, e^{i\pi/4}w_{30}\right)$
4	$\left(\frac{\sqrt{70}}{14}\, w_{40}, -\frac{\sqrt{7}}{2}\, e^{i\pi/4}w_{42}, w_{42}, \frac{1}{2}\, e^{-i\pi/4}w_{42}, w_{40}, \frac{1}{2}\, e^{i\pi/4}w_{42}, -w_{42}, -\frac{\sqrt{7}}{2}\, e^{-i\pi/4}w_{42}, \frac{\sqrt{70}}{14}\, w_{40}\right)$

C. Irreducible representations of the little groups

In the CM frame, the symmetry group of the cubic lattice is the cubic group O for particles with integer spin, and its double cover group ${}^2O$ for particles with half-integer spin. The group O consists of 24 elements R_i, *i.e.* rotation matrices, which are characterized by the axis $\boldsymbol{n}^{(i)}$ and angle ω_i of rotation (with $i = 1, \cdots, 24$). The rotation matrices are given by

$$(R_i)_{\alpha\beta} = \cos\omega_i\,\delta_{\alpha\beta} + (1-\cos\omega_i)\,n_\alpha^{(i)} n_\beta^{(i)} - \sin\omega_i\,\epsilon_{\alpha\beta\gamma}\,n_\gamma^{(i)}\,, \quad \alpha,\beta,\gamma = 1,2,3\,. \tag{49}$$

The 24 elements of O fall into five different conjugacy classes. They are listed in Table I. The group ${}^2O$ has 48 elements R_i. As for O, they are characterized by the axis $\boldsymbol{n}^{(i)}$ and angle ω_i (with $i = 1, \cdots, 48$ now). The 48 elements of ${}^2O$ fall into eight different conjugacy classes. They are listed in Table II.

The full symmetry group includes space inversions I, which commute with the elements of O and ${}^2O$. Choosing $T(I) = -1$,[1] where $T(I)$ denotes an element of any matrix representation of I, the elements of O and ${}^2O$ combined with I form the product groups $O_h = O \otimes \{1, -1\}$ and ${}^2O_h = {}^2O \otimes \{1, -1\}$, respectively. Irreducible matrix representations of O_h and ${}^2O_h$ have been given, for example, in [12].

In the CM frame moving with velocity $\boldsymbol{v} = \boldsymbol{P}/W$, $\boldsymbol{P} = (2\pi/L)\,\boldsymbol{d}$ in the laboratory frame, the symmetry group reduces to certain subgroups of O_h and ${}^2O_h$, hereafter referred to as the little groups. In the case of unequal masses, the little group consists of elements $S_i = \{R_i, IR_i\} \in O_h$ and ${}^2O_h$, respectively, which obey

$$S_i\,\boldsymbol{d} = \boldsymbol{d}\,. \tag{50}$$

In the case of equal masses, the system is symmetric under $\boldsymbol{d} \to -\boldsymbol{d}$, and the little group consists of elements S_i, which obey

$$S_i\,\boldsymbol{d} = \pm\boldsymbol{d}\,. \tag{51}$$

In Table III we list the elements $R_i \in O$ and ${}^2O$ that satisfy the condition $R_i\,\boldsymbol{d} = \boldsymbol{d}$ and $R_i\,\boldsymbol{d} = -\boldsymbol{d}$ for our three choices of $\boldsymbol{d}$, together with the corresponding little groups. With $I\boldsymbol{d} = -\boldsymbol{d}$, the action of the group elements S_i on $\boldsymbol{d}$ is now fully defined.

[1] Alternatively, we could have chosen $T(I) = 1$. Both choices are consistent with $I^2 = 1$.

Class	i	$\boldsymbol{n}^{(i)}$	ω_i
I	1	any	0
$8C_3$	2	$(1,1,1)/\sqrt{3}$	$-2\pi/3$
	3	$(1,1,1)/\sqrt{3}$	$2\pi/3$
	4	$(-1,1,1)/\sqrt{3}$	$-2\pi/3$
	5	$(-1,1,1)/\sqrt{3}$	$2\pi/3$
	6	$(-1,-1,1)/\sqrt{3}$	$-2\pi/3$
	7	$(-1,-1,1)/\sqrt{3}$	$2\pi/3$
	8	$(1,-1,1)/\sqrt{3}$	$-2\pi/3$
	9	$(1,-1,1)/\sqrt{3}$	$2\pi/3$
$6C_4$	10	$(1,0,0)$	$-\pi/2$
	11	$(1,0,0)$	$\pi/2$
	12	$(0,1,0)$	$-\pi/2$
	13	$(0,1,0)$	$\pi/2$
	14	$(0,0,1)$	$-\pi/2$
	15	$(0,0,1)$	$\pi/2$
$6C_2'$	16	$(0,1,1)/\sqrt{2}$	$-\pi$
	17	$(0,-1,1)/\sqrt{2}$	$-\pi$
	18	$(1,1,0)/\sqrt{2}$	$-\pi$
	19	$(1,-1,0)/\sqrt{2}$	$-\pi$
	20	$(1,0,1)/\sqrt{2}$	$-\pi$
	21	$(-1,0,1)/\sqrt{2}$	$-\pi$
$3C_2$	22	$(1,0,0)$	$-\pi$
	23	$(0,1,0)$	$-\pi$
	24	$(0,0,1)$	$-\pi$

TABLE I: The elements of the cubic group, parameterized by the rotation axis $\boldsymbol{n}^{(i)}$ and rotation angle ω_i, divided into the different conjugacy classes.

Class	i	$\boldsymbol{n}^{(i)}$	ω_i
I	1	any	0
$6C_4$	2	$(1,0,0)$	π
	3	$(0,1,0)$	π
	4	$(0,0,1)$	π
	5	$(1,0,0)$	$-\pi$
	6	$(0,1,0)$	$-\pi$
	7	$(0,0,1)$	$-\pi$
$6C_8'$	8	$(1,0,0)$	$\pi/2$
	9	$(0,1,0)$	$\pi/2$
	10	$(0,0,1)$	$\pi/2$
	11	$(1,0,0)$	$-\pi/2$
	12	$(0,1,0)$	$-\pi/2$
	13	$(0,0,1)$	$-\pi/2$
$6C_8$	14	$(1,0,0)$	$3\pi/2$
	15	$(0,1,0)$	$3\pi/2$
	16	$(0,0,1)$	$3\pi/2$
	17	$(1,0,0)$	$-3\pi/2$
	18	$(0,1,0)$	$-3\pi/2$
	19	$(0,0,1)$	$-3\pi/2$
$8C_6$	20	$(1,1,1)/\sqrt{3}$	$2\pi/3$
	21	$(-1,1,1)/\sqrt{3}$	$2\pi/3$
	22	$(-1,-1,1)/\sqrt{3}$	$2\pi/3$
	23	$(1,-1,1)/\sqrt{3}$	$2\pi/3$
	24	$(1,1,1)/\sqrt{3}$	$-2\pi/3$
	25	$(-1,1,1)/\sqrt{3}$	$-2\pi/3$
	26	$(-1,-1,1)/\sqrt{3}$	$-2\pi/3$
	27	$(1,-1,1)/\sqrt{3}$	$-2\pi/3$

Class	i	$\boldsymbol{n}^{(i)}$	ω_i
$8C_3$	28	$(1,1,1)/\sqrt{3}$	$4\pi/3$
	29	$(-1,1,1)/\sqrt{3}$	$4\pi/3$
	30	$(-1,-1,1)/\sqrt{3}$	$4\pi/3$
	31	$(1,-1,1)/\sqrt{3}$	$4\pi/3$
	32	$(1,1,1)/\sqrt{3}$	$-4\pi/3$
	33	$(-1,1,1)/\sqrt{3}$	$-4\pi/3$
	34	$(-1,-1,1)/\sqrt{3}$	$-4\pi/3$
	35	$(1,-1,1)/\sqrt{3}$	$-4\pi/3$
$12C_4'$	36	$(0,1,1)/\sqrt{2}$	π
	37	$(0,-1,1)/\sqrt{2}$	π
	38	$(1,1,0)/\sqrt{2}$	π
	39	$(1,-1,0)/\sqrt{2}$	π
	40	$(1,0,1)/\sqrt{2}$	π
	41	$(-1,0,1)/\sqrt{2}$	π
	42	$(0,1,1)/\sqrt{2}$	$-\pi$
	43	$(0,-1,1)/\sqrt{2}$	$-\pi$
	44	$(1,1,0)/\sqrt{2}$	$-\pi$
	45	$(1,-1,0)/\sqrt{2}$	$-\pi$
	46	$(1,0,1)/\sqrt{2}$	$-\pi$
	47	$(-1,0,1)/\sqrt{2}$	$-\pi$
J	48	any	2π

TABLE II: The elements of the double cover group of the cubic group, parameterized by the rotation axis $\boldsymbol{n}^{(i)}$ and rotation angle ω_i, divided into the different conjugacy classes.

Group	$\boldsymbol{d}$	Little Group	$R_i\,\boldsymbol{d}=\boldsymbol{d}$	$R_i\,\boldsymbol{d}=-\boldsymbol{d}$
O_h	$(0,0,1)$	C_{4v}	$\{R_i \vert i=1,14,15,24\}$	$\{R_i \vert i=18,19,22,23\}$
	$(1,1,0)$	C_{2v}	$\{R_i \vert i=1,18\}$	$\{R_i \vert i=19,24\}$
	$(1,1,1)$	C_{3v}	$\{R_i \vert i=1,2,3\}$	$\{R_i \vert i=17,19,21\}$
${}^2O_h$	$(0,0,1)$	${}^2C_{4v}$	$\{R_i \vert i=1,4,7,10,13,16,19,48\}$	$\{R_i \vert i=2,3,5,6,38,39,44,45\}$
	$(1,1,0)$	${}^2C_{2v}$	$\{R_i \vert i=1,38,44,48\}$	$\{R_i \vert i=4,7,39,45\}$
	$(1,1,1)$	${}^2C_{3v}$	$\{R_i \vert i=1,20,24,28,32,48\}$	$\{R_i \vert i=37,39,41,43,45,47\}$

TABLE III: Rotations R_i that obey the condition $R_i\,\boldsymbol{d}=\pm\boldsymbol{d}$.

As we shall see, several of the irreducible representations of the little groups C_{4v}, ${}^2C_{4v}$, ${}^2C_{2v}$, C_{3v} and ${}^2C_{3v}$ in Table III, namely E, G_1 and G_2, are two-dimensional. Two-dimensional representations G_1 and G_2 can be built from the matrices

$$(Y_i)_{\alpha\beta}=\left(e^{-\frac{i}{2}\,\boldsymbol{n}^{(i)}\boldsymbol{\sigma}\,\omega_i}\right)_{\alpha\beta}=\delta_{\alpha\beta}\,\cos\frac{\omega_i}{2}-i\,\left(\boldsymbol{n}^{(i)}\boldsymbol{\sigma}\right)_{\alpha\beta}\sin\frac{\omega_i}{2}\,,\quad \alpha,\beta=1,2 \tag{52}$$

with $i=1,\cdots,48$.

For the two-dimensional representation E in the bosonic case, it is convenient to introduce the matrices

$$\begin{aligned} &X_1=\mathbb{1}\,,\quad X_2=-\frac{1}{2}\,\mathbb{1}+i\frac{\sqrt{3}}{2}\,\sigma_2\,,\quad X_3=-\frac{1}{2}\,\mathbb{1}-i\frac{\sqrt{3}}{2}\,\sigma_2\,,\quad X_4=-\frac{1}{2}\,\sigma_3-\frac{\sqrt{3}}{2}\,\sigma_1\,,\\ &X_5=\sigma_3\,,\quad X_6=-\frac{1}{2}\,\sigma_3+\frac{\sqrt{3}}{2}\,\sigma_1\,,\quad X_7=i\frac{1}{\sqrt{2}}\,(\sigma_1+\sigma_2)\,,\quad X_8=\frac{1}{\sqrt{2}}\,(\sigma_1-\sigma_2)\,. \end{aligned} \tag{53}$$

In Tables IV, V, VI, VII, VIII, IX, we list the elements $\{S_i\}$ of the little groups C_{4v}, ${}^2C_{4v}$, ${}^2C_{2v}$, C_{3v} and ${}^2C_{3v}$, broken into the various conjugacy classes, the irreducible representations Γ and characters $\chi(\Gamma)$ of the little groups. Note that the rotation matrices R_i are specified by the rotation axes $\boldsymbol{n}^{(i)}$ and angles ω_i given in Tables I and II for the bosonic and fermionic case, respectively. In the case of the two-dimensional representations, we additionally list the matrices X_i, Y_i corresponding to the respective group elements. It is straightforward to check that these matrices obey the group multiplication laws. Later on we will need the whole information communicated in the tables for the construction of basis vectors and operators that transform according to the individual irreducible representations.

The results hold for the general case of unequal masses. For equal masses (integer spin) the representations are merely 'doubled'. Let us explain this by giving a specific example.

$\{S_i\}$	R_1	$\{R_{14}, R_{15}\}$	$\{IR_{18}, IR_{19}\}$	$\{IR_{22}, IR_{23}\}$	R_{24}
Γ \ Class	I	$2C_4$	$2IC_2'$	$2IC_2$	C_2
A_1	1	1	1	1	1
A_2	1	1	-1	-1	1
B_1	1	-1	-1	1	1
B_2	1	-1	1	-1	1
E	2	0	0	0	-2
E	X_1	$\{-X_7, X_7\}$	$\{X_5, -X_5\}$	$\{X_8, -X_8\}$	$-X_1$

TABLE IV: Character table of the little group C_{4v} for integer spin. The top row shows the elements of C_{4v} divided into conjugacy classes. The bottom row shows the corresponding matrices for the two-dimensional irreducible representation E. The rows in between list the characters of the various irreducible representations Γ of C_{4v}.

$\{S_i\}$	R_1	$\{R_4, R_7\}$	$\{R_{10}, R_{13}\}$	$\{R_{16}, R_{19}\}$	$\{IR_2, IR_3, IR_5, IR_6\}$	$\{IR_{38}, IR_{39}, IR_{44}, IR_{45}\}$	R_{48}
Γ \ Class	I	$2C_4$	$2C_8'$	$2C_8$	$4IC_4$	$4IC_4'$	J
A_1	1	1	1	1	1	1	1
A_2	1	1	1	1	-1	-1	1
B_1	1	1	-1	-1	1	-1	1
B_2	1	1	-1	-1	-1	1	1
E	2	-2	0	0	0	0	2
G_1	2	0	$\sqrt{2}$	$-\sqrt{2}$	0	0	-2
G_2	2	0	$-\sqrt{2}$	$\sqrt{2}$	0	0	-2
E	$\mathbb{1}$	$\{-\mathbb{1}, -\mathbb{1}\}$	$\{i\sigma_3, -i\sigma_3\}$	$\{-i\sigma_3, i\sigma_3\}$	$\{\sigma_1, -\sigma_1, \sigma_1, -\sigma_1\}$	$\{-\sigma_2, \sigma_2, -\sigma_2, \sigma_2\}$	$\mathbb{1}$
G_1	Y_1	$\{Y_4, Y_7\}$	$\{Y_{10}, Y_{13}\}$	$\{Y_{16}, Y_{19}\}$	$\{-Y_2, -Y_3, -Y_5, -Y_6\}$	$\{-Y_{38}, -Y_{39}, -Y_{44}, -Y_{45}\}$	Y_{48}
G_2	Y_1	$\{Y_4, Y_7\}$	$\{-Y_{10}, -Y_{13}\}$	$\{-Y_{16}, -Y_{19}\}$	$\{Y_2, Y_3, Y_5, Y_6\}$	$\{-Y_{38}, -Y_{39}, -Y_{44}, -Y_{45}\}$	Y_{48}

TABLE V: The same as Table IV for the little group ${}^2C_{4v}$ and half-integer spin, together with the matrices of the two-dimensional irreducible representations E, G_1 and G_2.

S_i	R_1	R_{18}	IR_{19}	IR_{24}
Class / Γ	I	C_2'	IC_2'	IC_2
A_1	1	1	1	1
A_2	1	1	-1	-1
B_1	1	-1	1	-1
B_2	1	-1	-1	1

TABLE VI: The same as Table IV for the little group C_{2v} and integer spin.

$\{S_i\}$	R_1	$\{R_{38}, R_{44}\}$	$\{IR_4, IR_7\}$	$\{IR_{39}, IR_{45}\}$	R_{48}
Class / Γ	I	$2C_4'$	$4IC_4$	$4IC_4'$	J
A_1	1	1	1	1	1
A_2	1	1	-1	-1	1
B_1	1	-1	-1	1	1
B_2	1	-1	1	-1	1
G_1	2	0	0	0	-2
G_1	Y_1	$\{Y_{38}, Y_{44}\}$	$\{-Y_4, -Y_7\}$	$\{-Y_{39}, -Y_{45}\}$	Y_{48}

TABLE VII: The same as Table IV for the little group ${}^2C_{2v}$ and half-integer spin, together with the matrices of the two-dimensional irreducible representation G_1.

$\{S_i\}$	R_1	$\{R_2, R_3\}$	$\{IR_{17}, IR_{19}, IR_{21}\}$
Class / Γ	I	$2C_3$	$3IC_2'$
A_1	1	1	1
A_2	1	1	-1
E	2	-1	0
E	X_1	$\{X_2, X_3\}$	$\{-X_4, -X_5, -X_6\}$

TABLE VIII: The same as Table IV for the little group C_{3v} and integer spin, together with the matrices of the two-dimensional irreducible representation E.

$\{S_i\}$	R_1	$\{R_{20}, R_{24}\}$	$\{R_{28}, R_{32}\}$	$\{IR_{37}, IR_{45}, IR_{47}\}$	$\{IR_{39}, IR_{41}, IR_{43}\}$	R_{48}
Class / Γ	I	$2C_6$	$2C_3$	$3IC_4$	$3IC_4'$	J
A_1	1	1	1	1	1	1
A_2	1	1	1	-1	-1	1
K_1	1	-1	1	i	$-i$	-1
K_2	1	-1	1	$-i$	i	-1
E	2	-1	-1	0	0	2
G_1	2	1	-1	0	0	-2
E	X_1	$\{X_3, X_2\}$	$\{X_2, X_3\}$	$\{-X_4, -X_5, -X_6\}$	$\{-X_5, -X_6, -X_4\}$	X_1
G_1	Y_1	$\{Y_{20}, Y_{24}\}$	$\{Y_{28}, Y_{32}\}$	$\{-Y_{37}, -Y_{45}, -Y_{47}\}$	$\{-Y_{39}, -Y_{41}, -Y_{43}\}$	Y_{48}

TABLE IX: The same as Table IV for the little group ${}^2C_{3v}$ and half-integer spin, together with the matrices of the two-dimensional irreducible representation E and G_1.

Consider the representation A_1 in Table IV. For equal masses two representations emerge: A_1^+ corresponding to $T(S) = 1$ for $S = R_1,\ R_{14},\ R_{15},\ R_{24},\ R_{18},\ R_{19},\ R_{22},\ R_{23},\ IR_1,\ IR_{14},\ IR_{15},\ IR_{24},\ IR_{18},\ IR_{19},\ IR_{22},\ IR_{23}$, and A_1^- corresponding to $T(S) = 1$ for $S = R_1,\ R_{14},\ R_{15},\ R_{24},\ IR_{18},\ IR_{19},\ IR_{22},\ IR_{23}$ and $T(S) = -1$ for $S = IR_1,\ IR_{14},\ IR_{15},\ IR_{24},\ R_{18},\ R_{19},\ R_{22},\ R_{23}$. All other representations are 'doubled' in a similar manner.

V. PHASE SHIFTS

From now on we shall drop the superscript $\boldsymbol{\Delta}$ from the matrix M. Following [12], the scattering phase shifts δ are obtained from the determinant equation

$$\det\,(M_{lm,l'm'} - \delta_{ll'}\delta_{mm'}\cot\delta_l) = 0 \tag{54}$$

for meson resonances and

$$\det\,(M_{Jl\mu,J'l'\mu'} - \delta_{JJ'}\delta_{ll'}\delta_{\mu\mu'}\cot\delta_{Jl}) = 0 \tag{55}$$

for baryon resonances. Equations (54) and (55) relate the phases δ in the infinite volume to the energy levels of the lattice Hamiltonian in a finite cubic box.

A. Reduction of the phase shift formulae

In the infinite volume, the basis vectors of an irreducible representation D^l of the rotation group of total angular momentum l are given by $|lm\rangle$ with $M_{lm,l'm'} = \langle lm|\hat{M}|l'm'\rangle$. In case of half-integer spin, the basis vectors are given by

$$|Jl\mu\rangle = \sum_{m,\sigma} |lm,\frac{1}{2}\sigma\rangle\langle lm,\frac{1}{2}\sigma|J\mu\rangle \tag{56}$$

with

$$M_{Jl\mu,J'l'\mu'} = \langle Jl\mu|\hat{M}|J'l'\mu'\rangle\,, \tag{57}$$

where $\mu = -J,\ldots,+J$ and $l = J \pm \frac{1}{2}$. The vectors $|lm\rangle$ and $|Jl\mu\rangle$ are parity eigenstates with parity $(-1)^l$.

In the case of the moving frame the basis vectors of an irreducible representation Γ can be written as

$$|\Gamma\alpha ln\rangle = \sum_m c^{\Gamma\alpha n}_{lm}|lm\rangle \tag{58}$$

for integer spin and

$$|\Gamma\alpha Jln\rangle = \sum_\mu c^{\Gamma\alpha n}_{Jl\mu}|Jl\mu\rangle \tag{59}$$

for half-integer spin, where α runs from 1 to the dimension of Γ, and n runs from 1 to $N(\Gamma,l)$, the number of occurrences of the irreducible representation Γ in D^l. The basis vectors of the various frames and representations are given in Tables X, XI, XII, XIII, XIV,

Γ	l	α	Basis vectors
A_1	0		$\|0,0\rangle$
A_1	1		$\|1,0\rangle$
E	1	1	$\frac{1}{2}(1-i)\|1,-1\rangle - \frac{1}{2}(1+i)\|1,1\rangle$
		2	$-\frac{1}{\sqrt{2}}i\|1,-1\rangle + \frac{1}{\sqrt{2}}\|1,1\rangle$
A_1	2		$\|2,0\rangle$
B_1	2		$\frac{1}{\sqrt{2}}(\|2,-2\rangle + \|2,2\rangle)$
B_2	2		$\frac{1}{\sqrt{2}}(\|2,-2\rangle - \|2,2\rangle)$
E	2	1	$\frac{1}{\sqrt{2}}\|2,-1\rangle - \frac{1}{\sqrt{2}}i\|2,1\rangle$
		2	$\frac{1}{2}(1-i)\|2,-1\rangle + \frac{1}{2}(1+i)\|2,1\rangle$

TABLE X: The basis vectors of the irreducible representations Γ of the little group C_{4v} and integer spin. α labels the components of the basis vectors of the two-dimensional representation E.

Γ	J	l	α	Basis vectors
G_1	$\frac{1}{2}$	0	1	$\|\frac{1}{2},\frac{1}{2}\rangle$
			2	$-\|\frac{1}{2},-\frac{1}{2}\rangle$
G_1	$\frac{1}{2}$	1	1	$\|\frac{1}{2},\frac{1}{2}\rangle$
			2	$\|\frac{1}{2},-\frac{1}{2}\rangle$
G_1	$\frac{3}{2}$	1	1	$\|\frac{3}{2},\frac{1}{2}\rangle$
			2	$-\|\frac{3}{2},-\frac{1}{2}\rangle$
G_2	$\frac{3}{2}$	1	1	$\|\frac{3}{2},-\frac{3}{2}\rangle$
			2	$\|\frac{3}{2},\frac{3}{2}\rangle$
G_1	$\frac{3}{2}$	2	1	$\|\frac{3}{2},\frac{1}{2}\rangle$
			2	$\|\frac{3}{2},-\frac{1}{2}\rangle$
G_2	$\frac{3}{2}$	2	1	$\|\frac{3}{2},-\frac{3}{2}\rangle$
			2	$-\|\frac{3}{2},\frac{3}{2}\rangle$

TABLE XI: The basis vectors of the irreducible representations Γ of the little group ${}^2C_{4v}$ and half-integer spin. α labels the components of the basis vectors of the two-dimensional representations G_1 and G_2.

Γ	l	Basis vectors
A_1	0	$\|0,0\rangle$
A_1	1	$\frac{1}{\sqrt{2}}(-i\|1,-1\rangle + \|1,1\rangle)$
B_1	1	$\|1,0\rangle$
B_2	1	$\frac{1}{\sqrt{2}}(i\|1,-1\rangle + \|1,1\rangle)$
A_1	2	$\|2,0\rangle$
A_1	2	$\frac{1}{\sqrt{2}}(\|2,-2\rangle - \|2,2\rangle)$
A_2	2	$\frac{1}{\sqrt{2}}(\|2,-1\rangle - i\|2,1\rangle)$
B_1	2	$\frac{1}{\sqrt{2}}(\|2,-1\rangle + i\|2,1\rangle)$
B_2	2	$\frac{1}{\sqrt{2}}(\|2,-2\rangle + \|2,2\rangle)$

TABLE XII: The basis vectors of the irreducible representations Γ of the little group C_{2v} and integer spin.

Γ	J	l	α	Basis vectors
G_1	$\frac{1}{2}$	0	1	$\|\frac{1}{2},-\frac{1}{2}\rangle$
			2	$-i\|\frac{1}{2},\frac{1}{2}\rangle$
G_1	$\frac{1}{2}$	1	1	$\|\frac{1}{2},\frac{1}{2}\rangle$
			2	$\|\frac{1}{2},-\frac{1}{2}\rangle$
G_1	$\frac{3}{2}$	1	1	$\|\frac{3}{2},-\frac{3}{2}\rangle$
			2	$\|\frac{3}{2},\frac{3}{2}\rangle$
G_1	$\frac{3}{2}$	1	1	$-\|\frac{3}{2},\frac{1}{2}\rangle$
			2	$\|\frac{3}{2},-\frac{1}{2}\rangle$
G_1	$\frac{3}{2}$	2	1	$i\|\frac{3}{2},\frac{3}{2}\rangle$
			2	$\|\frac{3}{2},-\frac{3}{2}\rangle$
G_1	$\frac{3}{2}$	2	1	$\|\frac{3}{2},-\frac{1}{2}\rangle$
			2	$i\|\frac{3}{2},\frac{1}{2}\rangle$

TABLE XIII: The basis vectors of the irreducible representations Γ of the little group ${}^2C_{2v}$ and half-integer spin. α labels the components of the basis vectors of the two-dimensional representation G_1.

Γ	l	α	Basis vectors
A_1	0		$\|0,0\rangle$
A_1	1		$-\frac{1}{\sqrt{3}}i\|1,-1\rangle - \frac{1}{\sqrt{6}}(1+i)\|1,0\rangle + \frac{1}{\sqrt{3}}\|1,1\rangle$
E	1	1	$\frac{1}{\sqrt{2}}i\|1,-1\rangle + \frac{1}{\sqrt{2}}\|1,1\rangle$
		2	$-\frac{1}{\sqrt{6}}\|1,-1\rangle + \frac{1}{\sqrt{3}}(1-i)\|1,0\rangle - \frac{1}{\sqrt{6}}i\|1,1\rangle$
A_1	2		$\frac{1}{\sqrt{6}}\|2,-2\rangle + \frac{1}{\sqrt{6}}(1-i)\|2,-1\rangle + \frac{1}{\sqrt{6}}(1+i)\|2,1\rangle - \frac{1}{\sqrt{6}}\|2,2\rangle$
E	2	1	$\frac{1}{\sqrt{2}}\|2,-2\rangle + \frac{1}{\sqrt{2}}\|2,2\rangle$
		2	$-\|2,0\rangle$
E	2	1	$\frac{1}{\sqrt{2}}\|2,-1\rangle - \frac{1}{\sqrt{2}}i\|2,1\rangle$
		2	$-\frac{1}{\sqrt{6}}(1-i)\|2,-2\rangle - \frac{1}{\sqrt{6}}i\|2,-1\rangle + \frac{1}{\sqrt{6}}\|2,1\rangle + \frac{1}{\sqrt{6}}(1-i)\|2,2\rangle$

TABLE XIV: The basis vectors of the irreducible representations Γ of the little group C_{3v} and integer spin. α labels the components of the basis vectors of the two-dimensional representation E.

Γ	J	l	α	Basis vectors
G_1	$\frac{1}{2}$	0	1	$\frac{\sqrt{6}}{3}\|\frac{1}{2},-\frac{1}{2}\rangle + \frac{1}{\sqrt{6}}(1-i)\|\frac{1}{2},\frac{1}{2}\rangle$
			2	$-\frac{1}{\sqrt{6}}(1-i)\|\frac{1}{2},-\frac{1}{2}\rangle - \frac{\sqrt{6}}{3}i\|\frac{1}{2},\frac{1}{2}\rangle$
G_1	$\frac{1}{2}$	1	1	$\|\frac{1}{2},\frac{1}{2}\rangle$
			2	$\|\frac{1}{2},-\frac{1}{2}\rangle$
G_1	$\frac{3}{2}$	1	1	$\frac{1}{\sqrt{6}}(1+i)\|\frac{3}{2},-\frac{3}{2}\rangle + \frac{1}{\sqrt{2}}\|\frac{3}{2},-\frac{1}{2}\rangle + \frac{1}{\sqrt{6}}i\|\frac{3}{2},\frac{3}{2}\rangle$
			2	$-\frac{1}{\sqrt{6}}\|\frac{3}{2},-\frac{3}{2}\rangle - \frac{1}{\sqrt{2}}i\|\frac{3}{2},\frac{1}{2}\rangle + \frac{1}{\sqrt{6}}(1+i)\|\frac{3}{2},\frac{3}{2}\rangle$
K_1	$\frac{3}{2}$	1		$-(\frac{\sqrt{3}}{6}(1+i) + \frac{\sqrt{6}}{12}(1-i))\|\frac{3}{2},-\frac{3}{2}\rangle + \frac{1}{2}\|\frac{3}{2},-\frac{1}{2}\rangle + \frac{\sqrt{2}}{4}(1+i)\|\frac{3}{2},\frac{1}{2}\rangle + (\frac{\sqrt{6}}{6} - \frac{\sqrt{3}}{6}i)\|\frac{3}{2},\frac{3}{2}\rangle$
K_2	$\frac{3}{2}$	1		$-(\frac{\sqrt{3}}{6}(1+i) - \frac{\sqrt{6}}{12}(1-i))\|\frac{3}{2},-\frac{3}{2}\rangle + \frac{1}{2}\|\frac{3}{2},-\frac{1}{2}\rangle - \frac{\sqrt{2}}{4}(1+i)\|\frac{3}{2},\frac{1}{2}\rangle - (\frac{\sqrt{6}}{6} + \frac{\sqrt{3}}{6}i)\|\frac{3}{2},\frac{3}{2}\rangle$
G_1	$\frac{3}{2}$	2	1	$\frac{1}{\sqrt{6}}\|\frac{3}{2},-\frac{1}{2}\rangle + \frac{1}{\sqrt{6}}(1-i)\|\frac{3}{2},\frac{1}{2}\rangle + \frac{1}{\sqrt{2}}i\|\frac{3}{2},\frac{3}{2}\rangle$
			2	$\frac{1}{\sqrt{2}}\|\frac{3}{2},-\frac{3}{2}\rangle + \frac{1}{\sqrt{6}}(1-i)\|\frac{3}{2},-\frac{1}{2}\rangle + \frac{1}{\sqrt{6}}i\|\frac{3}{2},\frac{1}{2}\rangle$
K_1	$\frac{3}{2}$	2		$-(\frac{\sqrt{3}}{6}(1+i) - \frac{\sqrt{6}}{12}(1-i))\|\frac{3}{2},-\frac{3}{2}\rangle + \frac{1}{2}\|\frac{3}{2},-\frac{1}{2}\rangle - \frac{\sqrt{2}}{4}(1+i)\|\frac{3}{2},\frac{1}{2}\rangle - (\frac{\sqrt{6}}{6} + \frac{\sqrt{3}}{6}i)\|\frac{3}{2},\frac{3}{2}\rangle$
K_2	$\frac{3}{2}$	2		$-(\frac{\sqrt{3}}{6}(1+i) + \frac{\sqrt{6}}{12}(1-i))\|\frac{3}{2},-\frac{3}{2}\rangle + \frac{1}{2}\|\frac{3}{2},-\frac{1}{2}\rangle + \frac{\sqrt{2}}{4}(1+i)\|\frac{3}{2},\frac{1}{2}\rangle + (\frac{\sqrt{6}}{6} - \frac{\sqrt{3}}{6}i)\|\frac{3}{2},\frac{3}{2}\rangle$

TABLE XV: The basis vectors of the irreducible representations Γ of the little group ${}^2C_{3v}$ and half-integer spin. α labels the components of the basis vectors of the two-dimensional representation G_1.

XV for $l = 0, 1$ and 2. The coefficients $c_{lm}^{\Gamma\alpha n}$ and $c_{Jl\mu}^{\Gamma\alpha n}$ can be directly read off from these tables.

The matrix elements of $\hat{M}$ in the new basis are given by

$$\langle \Gamma\alpha l n|\hat{M}|\Gamma'\alpha' l' n'\rangle = \sum_{mm'} c_{lm}^{\Gamma\alpha n\,*}\, c_{l'm'}^{\Gamma'\alpha' n'}\; M_{lm,l'm'} \tag{60}$$

for meson resonances and

$$\langle \Gamma\alpha Jl n|\hat{M}|\Gamma'\alpha' J' l' n'\rangle = \sum_{\mu\mu'} c_{Jl\mu}^{\Gamma\alpha n\,*}\, c_{J'l'\mu'}^{\Gamma'\alpha' n'}\; M_{Jl\mu,J'l'\mu'} \tag{61}$$

for baryon resonances.

According to Schur's lemma, $\hat{M}$ is partially diagonalized in the new basis,

$$\begin{aligned} \langle \Gamma\alpha l n|\hat{M}|\Gamma'\alpha' l' n'\rangle &= \delta_{\Gamma\Gamma'}\delta_{\alpha\alpha'} M^{\Gamma}_{ln,l'n'}\,, \\ \langle \Gamma\alpha Jl n|\hat{M}|\Gamma'\alpha' J' l' n'\rangle &= \delta_{\Gamma\Gamma'}\delta_{\alpha\alpha'} M^{\Gamma}_{Jln,J'l'n'}\,. \end{aligned} \tag{62}$$

The phase shift formulae (54) and (55) then reduce to

$$\begin{aligned} &\det\left(M^{\Gamma}_{ln,l'n'} - \delta_{ll'}\delta_{nn'}\,\cot\delta_l\,\right) = 0\,, \\ &\det\left(M^{\Gamma}_{Jln,J'l'n'} - \delta_{JJ'}\delta_{ll'}\delta_{nn'}\,\cot\delta_{Jl}\right) = 0\,. \end{aligned} \tag{63}$$

The partially diagonalized matrices $M^{\Gamma}_{ln,l'n'}$ and $M^{\Gamma}_{Jln,J'l'n'}$ are given below for $l \leq 2$ and $J = 1/2$ and $3/2$.

B. Reduced matrices M^{Γ}

1. $\boldsymbol{d} = (0, 0, 1)$ – *integer spin*

In this case $N(\Gamma, l) = 1$ for all representations, so that we may drop the subscripts n, n' from $M^{\Gamma}_{ln,l'n'}$. The matrices M^{Γ} have the following entries

$$\left(M^{\Gamma}_{l,l'}\right) = \begin{pmatrix} M_{0,0} & M_{0,1} & M_{0,2} \\ M_{1,0} & M_{1,1} & M_{1,2} \\ M_{2,0} & M_{2,1} & M_{2,2} \end{pmatrix} \tag{64}$$

with

$$M^{A_1} = \begin{pmatrix} w_{00} & \sqrt{3}iw_{10} & -\sqrt{5}w_{20} \\ -\sqrt{3}iw_{10} & w_{00} + 2w_{20} & i\frac{2\sqrt{15}}{5}w_{10} + i\frac{3\sqrt{15}}{5}w_{30} \\ -\sqrt{5}w_{20} & -i\frac{2\sqrt{15}}{5}w_{10} - i\frac{3\sqrt{15}}{5}w_{30} & w_{00} + \frac{10}{7}w_{20} + \frac{18}{7}w_{40} \end{pmatrix}, \tag{65}$$

$$M^{B_1} = \begin{pmatrix} 0 & 0 & 0 \\ 0 & 0 & 0 \\ 0 & 0 & w_{00} - \frac{10}{7} w_{20} + \frac{3}{7} w_{40} + \frac{3\sqrt{70}}{7} w_{44} \end{pmatrix}, \tag{66}$$

$$\mathcal{M}^{B_2} = \begin{pmatrix} 0 & 0 & 0 \\ 0 & 0 & 0 \\ 0 & 0 & w_{00} - \frac{10}{7} w_{20} + \frac{3}{7} w_{40} - \frac{3\sqrt{70}}{7} w_{44} \end{pmatrix}, \tag{67}$$

$$M^{E} = \begin{pmatrix} 0 & 0 & 0 \\ 0 & w_{00} - w_{20} & -\frac{3\sqrt{10}}{10}(1-i)(w_{10} - w_{30}) \\ 0 & -\frac{3\sqrt{10}}{10}(1+i)(w_{10} - w_{30}) & w_{00} + \frac{5}{7} w_{20} - \frac{12}{7} w_{40} \end{pmatrix}. \tag{68}$$

2. $\boldsymbol{d} = (0, 0, 1)$ *– half-integer spin*

In this case $N(\Gamma, l) = 1$ for all representations, so that we may drop the subscripts n, n' again. The matrices M^{Γ} have the following entries

$$\left(M^{\Gamma}_{Jl,J'l'}\right) = \begin{pmatrix} M_{\frac{1}{2}0,\frac{1}{2}0} & M_{\frac{1}{2}0,\frac{1}{2}1} & M_{\frac{1}{2}0,\frac{3}{2}1} & M_{\frac{1}{2}0,\frac{3}{2}2} \\ M_{\frac{1}{2}1,\frac{1}{2}0} & M_{\frac{1}{2}1,\frac{1}{2}1} & M_{\frac{1}{2}1,\frac{3}{2}1} & M_{\frac{1}{2}1,\frac{3}{2}2} \\ M_{\frac{3}{2}1,\frac{1}{2}0} & M_{\frac{3}{2}1,\frac{1}{2}1} & M_{\frac{3}{2}1,\frac{3}{2}1} & M_{\frac{3}{2}1,\frac{3}{2}2} \\ M_{\frac{3}{2}2,\frac{1}{2}0} & M_{\frac{3}{2}2,\frac{1}{2}1} & M_{\frac{3}{2}2,\frac{3}{2}1} & M_{\frac{3}{2}2,\frac{3}{2}2} \end{pmatrix} \tag{69}$$

with

$$M^{G_1} = \begin{pmatrix} w_{00} & i w_{10} & i\sqrt{2} w_{10} & -\sqrt{2} w_{20} \\ -i w_{10} & w_{00} & \sqrt{2} w_{20} & i\sqrt{2} w_{10} \\ -i\sqrt{2} w_{10} & \sqrt{2} w_{20} & w_{00} + w_{20} & \frac{i}{5} w_{10} + \frac{9i}{5} w_{30} \\ -\sqrt{2} w_{20} & -i\sqrt{2} w_{10} & -\frac{i}{5} w_{10} - \frac{9i}{5} w_{30} & w_{00} + w_{20} \end{pmatrix}, \tag{70}$$

$$M^{G_2} = \begin{pmatrix} 0 & 0 & 0 & 0 \\ 0 & 0 & 0 & 0 \\ 0 & 0 & w_{00} - w_{20} & i\frac{3}{5}(w_{10} - w_{30}) \\ 0 & 0 & -i\frac{3}{5}(w_{10} - w_{30}) & w_{00} - w_{20} \end{pmatrix}. \tag{71}$$

3. $\boldsymbol{d} = (1,1,0)$ – *integer spin*

The representation A_1 occurs twice in D^l for $l = 2$, $N(A_1, 2) = 2$. In all other cases $N(\Gamma, l) = 1$. The matrices M^Γ have the following entries

$$\left(M^\Gamma_{l[n],l'[n']}\right) = \begin{pmatrix} M_{0,0} & M_{0,1} & M_{0,21} & M_{0,22} \\ M_{1,0} & M_{1,1} & M_{1,21} & M_{1,22} \\ M_{21,0} & M_{21,1} & M_{21,21} & M_{21,22} \\ M_{22,0} & M_{22,1} & M_{22,21} & M_{22,22} \end{pmatrix} \tag{72}$$

with

$$\mathcal{M}^{A_1} = \begin{pmatrix} w_{00} & -\sqrt{6}(1-i)r_{11} & \sqrt{10}w_{22} & -\sqrt{5}w_{20} \\ -\sqrt{6}(1+i)r_{11} & A_{22} & A^-_{23} & A^+_{24} \\ -\sqrt{10}w_{22} & A^+_{23} & A_{33} & A_{34} \\ -\sqrt{5}w_{20} & A^-_{24} & -A_{34} & A_{44} \end{pmatrix}, \tag{73}$$

where $r_{js} = \operatorname{Re} w_{js}$ and

$$\begin{aligned} A^\pm_{23} &= \frac{3\sqrt{10}}{5}(1 \pm i)r_{11} - \frac{\sqrt{15}}{5}(1 \pm i)r_{31} - 3(1 \pm i)r_{33}\,, \\ A^\pm_{24} &= -\frac{\sqrt{30}}{5}(1 \pm i)r_{11} + \frac{6\sqrt{5}}{5}(1 \pm i)r_{31}\,, \\ A_{22} &= w_{00} - w_{20} - \sqrt{6}iw_{22}\,, \\ A_{33} &= w_{00} - \frac{10}{7}w_{20} + \frac{3}{7}w_{40} - \frac{3\sqrt{70}}{7}w_{44}\,, \\ A_{34} &= -\frac{10\sqrt{2}}{7}w_{22} + \frac{3\sqrt{30}}{7}w_{42}\,, \\ A_{44} &= w_{00} + \frac{10}{7}w_{20} + \frac{18}{7}w_{40}\,. \end{aligned} \tag{74}$$

For the remaining representations we drop the subscripts n, n' and obtain

$$M^{A_2} = \begin{pmatrix} 0 & 0 & 0 \\ 0 & 0 & 0 \\ 0 & 0 & w_{00} + \frac{5}{7}w_{20} - \frac{12}{7}w_{40} + \frac{5\sqrt{6}}{7}iw_{22} + \frac{6\sqrt{10}}{7}iw_{42} \end{pmatrix}, \tag{75}$$

$$M^{B_1} = \begin{pmatrix} 0 & 0 & 0 \\ 0 & w_{00} + 2w_{20} & -\frac{3\sqrt{10}}{5}(1+i)r_{11} - \frac{4\sqrt{15}}{5}(1+i)r_{31} \\ 0 & -\frac{3\sqrt{10}}{5}(1-i)r_{11} - \frac{4\sqrt{15}}{5}(1-i)r_{31} & B_{33} \end{pmatrix}, \tag{76}$$

$$M^{B_2} = \begin{pmatrix} 0 & 0 & 0 \\ 0 & w_{00} - w_{20} + \sqrt{6} i w_{22} & \tilde{B}^-_{23} \\ 0 & \tilde{B}^+_{23} & w_{00} - \frac{10}{7} w_{20} + \frac{3}{7} w_{40} + \frac{3\sqrt{70}}{4} w_{44} \end{pmatrix}, \tag{77}$$

where

$$\begin{aligned} B_{33} &= w_{00} + \frac{5}{7} w_{20} - \frac{12}{7} w_{40} - \frac{5\sqrt{6}}{7} i w_{22} - \frac{6\sqrt{10}}{7} i w_{42}\,, \\ \tilde{B}^{\pm}_{23} &= -\frac{3\sqrt{10}}{5}(1 \pm i) r_{11} + \frac{\sqrt{15}}{5}(1 \pm i) r_{31} - 3(1 \pm i) r_{33}\,. \end{aligned} \tag{78}$$

4. $\boldsymbol{d} = (1,1,0)$ – *half-integer spin*

In this case we are concerned with the representation G_1 only. We have $N(G_1, l) = 2$ for $J = \frac{3}{2}$ and $l = 1, 2$ and $N(G_1, l) = 1$ else. The matrix M^{G_1} has the following entries

$$\left(M^{G_1}_{Jl[n],J'l'[n']}\right) = \begin{pmatrix} M_{\frac{1}{2}0,\frac{1}{2}0} & M_{\frac{1}{2}0,\frac{1}{2}1} & M_{\frac{1}{2}0,\frac{3}{2}11} & M_{\frac{1}{2}0,\frac{3}{2}12} & M_{\frac{1}{2}0,\frac{3}{2}21} & M_{\frac{1}{2}0,\frac{3}{2}22} \\ M_{\frac{1}{2}1,\frac{1}{2}0} & M_{\frac{1}{2}1,\frac{1}{2}1} & M_{\frac{1}{2}1,\frac{3}{2}11} & M_{\frac{1}{2}1,\frac{3}{2}12} & M_{\frac{1}{2}1,\frac{3}{2}21} & M_{\frac{1}{2}1,\frac{3}{2}22} \\ M_{\frac{3}{2}11,\frac{1}{2}0} & M_{\frac{3}{2}11,\frac{1}{2}1} & M_{\frac{3}{2}11,\frac{3}{2}11} & M_{\frac{3}{2}11,\frac{3}{2}12} & M_{\frac{3}{2}11,\frac{3}{2}21} & M_{\frac{3}{2}11,\frac{3}{2}22} \\ M_{\frac{3}{2}12,\frac{1}{2}0} & M_{\frac{3}{2}12,\frac{1}{2}1} & M_{\frac{3}{2}12,\frac{3}{2}11} & M_{\frac{3}{2}12,\frac{3}{2}12} & M_{\frac{3}{2}12,\frac{3}{2}21} & M_{\frac{3}{2}12,\frac{3}{2}22} \\ M_{\frac{3}{2}21,\frac{1}{2}0} & M_{\frac{3}{2}21,\frac{1}{2}1} & M_{\frac{3}{2}21,\frac{3}{2}11} & M_{\frac{3}{2}21,\frac{3}{2}12} & M_{\frac{3}{2}21,\frac{3}{2}21} & M_{\frac{3}{2}21,\frac{3}{2}22} \\ M_{\frac{3}{2}22,\frac{1}{2}0} & M_{\frac{3}{2}22,\frac{1}{2}1} & M_{\frac{3}{2}22,\frac{3}{2}11} & M_{\frac{3}{2}22,\frac{3}{2}12} & M_{\frac{3}{2}22,\frac{3}{2}21} & M_{\frac{3}{2}22,\frac{3}{2}22} \end{pmatrix} \tag{79}$$

with

$$M^{G_1} = \begin{pmatrix} w_{00} & -\sqrt{2} G^-_{14} & -\sqrt{3} G^+_{14} & G^-_{14} & -2 i w_{22} & -\sqrt{2} w_{20} \\ -\sqrt{2} G^+_{14} & w_{00} & 2 w_{22} & \sqrt{2} w_{20} & -\sqrt{3} G^+_{14} & -G^+_{14} \\ -\sqrt{3} G^-_{14} & -2 w_{22} & w_{00} - w_{20} & \sqrt{2} w_{22} & G^-_{35} & G^-_{36} \\ G^+_{14} & \sqrt{2} w_{20} & -\sqrt{2} w_{22} & w_{00} + w_{20} & -G^+_{36} & G^+_{46} \\ -2 i w_{22} & -\sqrt{3} G^-_{14} & G^+_{35} & -G^-_{36} & w_{00} - w_{20} & -\sqrt{2} i w_{22} \\ -\sqrt{2} w_{20} & -G^-_{14} & G^+_{36} & G^-_{46} & -\sqrt{2} i w_{22} & w_{00} + w_{20} \end{pmatrix}, \tag{80}$$

where

$$
\begin{aligned}
G^{\pm}_{14} &= (1 \pm i) r_{11}\,, \\
G^{\pm}_{35} &= \frac{6\sqrt{5}}{5}(1 \pm i) r_{33}\,, \\
G^{\pm}_{36} &= -\frac{\sqrt{6}}{5}(1 \pm i)(r_{11} - \sqrt{6} r_{31})\,, \\
G^{\pm}_{46} &= -\frac{2\sqrt{2}}{5}(1 \pm i) r_{11} - \frac{6\sqrt{3}}{5}(1 \pm i) r_{31}\,.
\end{aligned}
\tag{81}
$$

5. $\boldsymbol{d} = (1,1,1)$ – *integer spin*

In this case we are concerned with two representations, A_1 and E. The representation A_1 occurs only once in D^l, and we find

$$
\begin{aligned}
M^{A_1} = \left(M^{A_1}_{l,l'}\right) &= \begin{pmatrix} M_{0,0} & M_{0,1} & M_{0,2} \\ M_{1,0} & M_{1,1} & M_{1,2} \\ M_{2,0} & M_{2,1} & M_{2,2} \end{pmatrix} \\
&= \begin{pmatrix} w_{00} & \frac{3\sqrt{2}}{2}(1-i) w_{10} & \sqrt{30} w_{22} \\ \frac{3\sqrt{2}}{2}(1+i) w_{10} & w_{00} - 2\sqrt{6} i w_{22} & \tilde{A}^{-}_{23} \\ -\sqrt{30} w_{22} & \tilde{A}^{+}_{23} & w_{00} - \frac{12}{7} w_{40} - \frac{12\sqrt{10}}{7} i w_{42} - \frac{10\sqrt{6}}{7} i w_{22} \end{pmatrix},
\end{aligned}
\tag{82}
$$

where

$$
\tilde{A}^{\pm}_{23} = -\frac{3\sqrt{10}}{5}(1 \pm i) w_{10} + \frac{3\sqrt{10}}{5}(1 \pm i) w_{30} \mp \sqrt{3}(1 \mp i) w_{32}\,. \tag{83}
$$

The representation E occurs twice in D^l for $l = 2$, $N(E,2) = 2$, and we obtain

$$
\begin{aligned}
M^{E} = \left(M^{E}_{l[n],l'[n']}\right) &= \begin{pmatrix} M_{0,0} & M_{0,1} & M_{0,21} & M_{0,22} \\ M_{1,0} & M_{1,1} & M_{1,21} & M_{1,22} \\ M_{21,0} & M_{21,1} & M_{21,21} & M_{21,22} \\ M_{22,0} & M_{22,1} & M_{22,21} & M_{22,22} \end{pmatrix} \\
&= \begin{pmatrix} 0 & 0 & 0 & 0 \\ 0 & w_{00} + i\sqrt{6} w_{22} & E^{-}_{23} & E_{24} \\ 0 & E^{+}_{23} & w_{00} + \frac{18}{7} w_{40} & E^{-}_{34} \\ 0 & E_{24} & -E^{+}_{34} & w_{00} - \frac{12}{7} w_{40} + \frac{6\sqrt{10}}{7} i w_{42} + \frac{5\sqrt{6}}{7} i w_{22} \end{pmatrix},
\end{aligned}
\tag{84}
$$

where

$$E_{23}^{\pm} = \frac{3\sqrt{5}}{5}(1 \pm i)w_{10} + \frac{9\sqrt{5}}{10}(1 \pm i)w_{30}\,,$$
$$E_{24} = \frac{3\sqrt{5}}{5}(w_{10} - w_{30}) + \sqrt{6}iw_{32}\,, \tag{85}$$
$$E_{34}^{\pm} = \frac{5\sqrt{6}}{7}(1 \pm i)w_{22} - \frac{9\sqrt{10}}{14}(1 \pm i)w_{42}\,.$$

6. $\boldsymbol{d} = (1,1,1)$ *– half-integer spin*

In this case $N(\Gamma, l) = 1$ for all representations. The matrices M^{Γ} have the following entries

$$\left(M^{\Gamma}_{Jl,J'l'}\right) = \begin{pmatrix} M_{\frac{1}{2}0,\frac{1}{2}0} & M_{\frac{1}{2}0,\frac{1}{2}1} & M_{\frac{1}{2}0,\frac{3}{2}1} & M_{\frac{1}{2}0,\frac{3}{2}2} \\ M_{\frac{1}{2}1,\frac{1}{2}0} & M_{\frac{1}{2}1,\frac{1}{2}1} & M_{\frac{1}{2}1,\frac{3}{2}1} & M_{\frac{1}{2}1,\frac{3}{2}2} \\ M_{\frac{3}{2}1,\frac{1}{2}0} & M_{\frac{3}{2}1,\frac{1}{2}1} & M_{\frac{3}{2}1,\frac{3}{2}1} & M_{\frac{3}{2}1,\frac{3}{2}2} \\ M_{\frac{3}{2}2,\frac{1}{2}0} & M_{\frac{3}{2}2,\frac{1}{2}1} & M_{\frac{3}{2}2,\frac{3}{2}1} & M_{\frac{3}{2}2,\frac{3}{2}2} \end{pmatrix} \tag{86}$$

with

$$M^{K_1} = \begin{pmatrix} 0 & 0 & 0 & 0 \\ 0 & 0 & 0 & 0 \\ 0 & 0 & w_{00} + \sqrt{6}iw_{22} & \bar{B}_{34}^{+} \\ 0 & 0 & \bar{B}_{34}^{-} & w_{00} + \sqrt{6}iw_{22} \end{pmatrix}, \tag{87}$$

where

$$\bar{B}_{34}^{\pm} = \left(-\frac{3\sqrt{2}}{5} \pm \frac{3}{5}i\right) w_{10} + \left(\frac{3\sqrt{2}}{5} \pm \frac{12}{5}i\right) w_{30} + \left(\pm\frac{\sqrt{30}}{5} - \frac{2\sqrt{15}}{5}i\right) w_{32}\,, \tag{88}$$

and

$$M^{K_2} = \begin{pmatrix} 0 & 0 & 0 & 0 \\ 0 & 0 & 0 & 0 \\ 0 & 0 & w_{00} + \sqrt{6}iw_{22} & \hat{B}_{34}^{+} \\ 0 & 0 & \hat{B}_{34}^{-} & w_{00} + \sqrt{6}iw_{22} \end{pmatrix}, \tag{89}$$

where

$$\hat{B}_{34}^{\pm} = \left(\frac{3\sqrt{2}}{5} \pm \frac{3}{5}i\right) w_{10} + \left(-\frac{3\sqrt{2}}{5} \pm \frac{12}{5}i\right) w_{30} + \left(\pm\frac{\sqrt{30}}{5} + \frac{2\sqrt{15}}{5}i\right) w_{32}\,, \tag{90}$$

and finally

$$M^{G_1} = \begin{pmatrix} w_{00} & \frac{\sqrt{6}}{2}(1-i)w_{10} & \sqrt{6}iw_{10} & -2\sqrt{3}iw_{22} \\ \frac{\sqrt{6}}{2}(1+i)w_{10} & w_{00} & \sqrt{6}(1+i)w_{22} & \sqrt{3}(1+i)w_{10} \\ -\sqrt{6}iw_{10} & -\sqrt{6}(1-i)w_{22} & w_{00}-i\sqrt{6}w_{22} & \tilde{G}_{34} \\ -2\sqrt{3}iw_{22} & \sqrt{3}(1-i)w_{10} & -\tilde{G}_{34} & w_{00}-i\sqrt{6}w_{22} \end{pmatrix}, \tag{91}$$

where

$$\tilde{G}_{34} = \frac{6\sqrt{3}}{5}iw_{30} - \frac{\sqrt{3}}{5}iw_{10} - \frac{3\sqrt{10}}{5}w_{32}\,. \tag{92}$$

VI. THREE EXAMPLES

Let us now apply the formulae derived above to a few concrete cases. A general feature of unequal mass particles is that spin and angular momentum mix under the Lorentz boost, which complicates the extraction of phase shifts significantly. In the case of baryon resonances, nonvanishing momenta prove most advantageous for the evaluation of P-wave phase shifts, as we have seen in the Introduction. For S-wave baryon resonances nonvanishing momenta are of no big advantage as far as moving the level crossing to smaller values of $m_\pi L$ is concerned.

Of primary interest are the ρ and the Δ resonance. The calculation of the mass and the width of the ρ meson provides a benchmark test, which has to be passed successfully before we can address more complex systems. The Δ resonance is interesting for two reasons. First

$\boldsymbol{d}$	Little Group	Γ	$\cot\delta_1$
$(0,0,1)$	C_{4v}	$A_1^\pm$	$w_{00}+2w_{20}$
		$E^\pm$	$w_{00}-w_{20}$
$(1,1,0)$	C_{2v}	$A_1^\pm$	$w_{00}-w_{20}-i\sqrt{6}w_{22}$
		$B_1^\pm$	$w_{00}+2w_{20}$
		$B_2^\pm$	$w_{00}-w_{20}+i\sqrt{6}w_{22}$
$(1,1,1)$	C_{3v}	$A_1^\pm$	$w_{00}-i2\sqrt{6}w_{22}$
		$E^\pm$	$w_{00}+i\sqrt{6}w_{22}$

TABLE XVI: The phase shifts of the ρ resonance for the various boost vectors and representations.

of all, it is one of the very few elastic two-body baryon resonances, and as such qualifies for a first extension of Lüscher's method to particles carrying spin. Secondly, being a P_{33} wave, its phase $\delta_{\frac{3}{2}1}$ can be computed directly from representations G_2 and B_1, B_2. Finally, we consider the $N^\star(1440)$ Roper resonance. Being a P_{11} wave and carrying spin 1/2, it couples to the representation G_1 only, which mixes spin 1/2 with spin 3/2 and angular momentum $l = 0$ with angular momentum $l = 1$.

A. The ρ resonance

In the case of equal masses and integer spin the situation simplifies significantly. All matrices M^Γ turn out to be diagonal, and the phase shifts can be directly read off from their eigenvalues. The phase shifts δ_1 of the ρ resonance are given in Table XVI.

B. The $\Delta(1232)$ resonance

Neglecting mixing with D waves (and higher), it is straightforward to compute $\delta_{\frac{3}{2}1}$ for boost vector $\boldsymbol{d} = (0, 0, 1)$ from the representation G_1 and for boost vector $\boldsymbol{d} = (1, 1, 1)$ from representations B_1 and B_2, giving

$\boldsymbol{d}$	Γ	$\cot \delta_{\frac{3}{2}1}$
$(0, 0, 1)$	G_2	$w_{00} - w_{20}$
$(1, 1, 1)$	B_1, B_2	$w_{00} + i\sqrt{6} w_{22}$

(93)

In all other cases $\delta_{\frac{3}{2}1}$ mixes with lower spin and lower partial waves.

The same formulae apply to the $\Sigma^*(1385)$ resonance (whose energy levels we have shown in Fig. 2), which is a P_{13} wave.

C. The $N^\star(1440)$ Roper resonance

Let us consider the boost vector $\boldsymbol{d} = (0, 0, 1)$ and representation G_1. Alternatively we could consider the boost vectors $\boldsymbol{d} = (1, 1, 0)$ and $\boldsymbol{d} = (1, 1, 1)$. Neglecting mixing with $J = \frac{3}{2}$ states for the moment, we need to solve

$$\begin{vmatrix} w_{00} - \cot \delta_{\frac{1}{2}0} & i\, w_{10} \\ -i\, w_{10} & w_{00} - \cot \delta_{\frac{1}{2}1} \end{vmatrix} = 0\,, \tag{94}$$

which leads to

$$\cot\delta_{\frac{1}{2}1}\,\cot\delta_{\frac{1}{2}0} - \left(\cot\delta_{\frac{1}{2}1} - \cot\delta_{\frac{1}{2}0}\right)\,w_{00} + w_{00}^2 - w_{10}^2 = 0\,. \tag{95}$$

The phase shift that interests us here is $\delta_{\frac{1}{2}1}$. To compute $\delta_{\frac{1}{2}1}$ from (95) we need to know $\delta_{\frac{1}{2}0}$, which is most easily obtained from eigenstates of zero total momentum, $\boldsymbol{d} = (0,0,0)$. It is not excluded that the spin-1/2 states mix with the P-wave spin-3/2 state, though no resonance of that kind has been reported by the Particle Data Group [13]. In this case we would have

$$\begin{vmatrix} w_{00} - \cot\delta_{\frac{1}{2}0} & i\,w_{10} & i\,\sqrt{2}\,w_{10} \\ -i\,w_{10} & w_{00} - \cot\delta_{\frac{1}{2}1} & \sqrt{2}\,w_{20} \\ -i\,\sqrt{2}\,w_{10} & \sqrt{2}\,w_{20} & w_{00} + w_{20} - \cot\delta_{\frac{3}{2}1} \end{vmatrix} = 0\,. \tag{96}$$

To find out, and to solve (96), the phase $\delta_{\frac{3}{2}1}$ can be directly computed from representation G_2. It has to be extrapolated to the appropriate value of q^2 though.

VII. OPERATORS

Recently, several authors [8, 14–16] have started to construct operators projecting onto selected irreducible representations of the little groups. In this Section we extend the work to higher representations and/or particles with spin.

We start from (generally nonlocal) operators $O_\alpha(\boldsymbol{x}_1, \boldsymbol{x}_2, t)$. Under space rotations $\hat{R}$ they transform like

$$(\hat{R}\,O)_\alpha(\boldsymbol{x}_1, \boldsymbol{x}_2, t) = S_{\alpha\beta}(R)\,O_\beta(R^{-1}\boldsymbol{x}_1, R^{-1}\boldsymbol{x}_2, t)\,, \tag{97}$$

where $R^{-1}\boldsymbol{x}$ denotes the rotated vector $\boldsymbol{x}$, and the matrices $S_{\alpha\beta}(R)$ form a linear representation of the group $SO(3)$ in case of integer spin and $SU(2)$ in case of half-integer spin. The explicit form of $S_{\alpha\beta}(R)$ is well known for scalar, vector and spinor fields. Under space inversions $\hat{I}$ the operators transform as

$$(\hat{I}\,O)_\alpha(\boldsymbol{x}_1, \boldsymbol{x}_2, t) = I_{\alpha\beta}\,O_\beta(-\boldsymbol{x}_1, -\boldsymbol{x}_2, t) \tag{98}$$

with $I^2 = 1$. An operator $O_\alpha^\Gamma(\boldsymbol{x}_1, \boldsymbol{x}_2, t)$, which transforms according to the irreducible representation Γ of the little group, is given by (see, for example, [17])

$$O_\alpha^\Gamma(\boldsymbol{x}_1, \boldsymbol{x}_2, t) = \sum_i \chi_\Gamma^*(S_i)\,(\hat{S}_i\,O)_\alpha(\boldsymbol{x}_1, \boldsymbol{x}_2, t)\,, \tag{99}$$

where the sum runs over all elements S_i of the little group, which are either pure rotations R_i, or rotations combined with space inversion $I\,R_i$. The quantities $\chi_\Gamma(S_i)$ denote the characters in the representation Γ. The operators can be trivially Fourier transformed to momentum space.

Below we will give a few examples of single-particle and two-particle operators, which demonstrate the procedure to be followed in the general case.

A. Single-particle operators

Let us start with the simple case of quark-antiquark and three-quark operators, and discuss this case in detail.

1. *The case* $\boldsymbol{d} = (0,0,1)$ *– scalar mesons*

Consider the operator

$$O(\boldsymbol{p},t) = \sum_{\boldsymbol{x}} e^{i\boldsymbol{p}\boldsymbol{x}}\, \bar{q}(\boldsymbol{x},t) q(\boldsymbol{x},t)\,. \tag{100}$$

Under rotations and space inversions the operator transforms as

$$\hat{R}\,(\bar{q}(\boldsymbol{x},t)q(\boldsymbol{x},t)) = \bar{q}(R^{-1}\boldsymbol{x},t)q(R^{-1}\boldsymbol{x},t)\,, \quad \hat{I}\,(\bar{q}(\boldsymbol{x},t)q(\boldsymbol{x},t)) = \bar{q}(-\boldsymbol{x},t)q(-\boldsymbol{x},t)\,. \tag{101}$$

The projected operator takes the form

$$O^\Gamma(\boldsymbol{p},t) = \sum_i \chi^*_\Gamma(S_i) \sum_{\boldsymbol{x}} e^{i\boldsymbol{p}\boldsymbol{x}}\, \bar{q}(S_i^{-1}\boldsymbol{x},t) q(S_i^{-1}\boldsymbol{x},t)\,. \tag{102}$$

Note that the sites $R_i^{-1}\boldsymbol{x}$ and $-\boldsymbol{x}$ belong to the lattice if $\boldsymbol{x}$ does. In the case of unequal masses, the momentum $\boldsymbol{p}$ is left invariant by the elements of the little group, $S_i\,\boldsymbol{p} = \boldsymbol{p}$, so that we have

$$O^\Gamma(\boldsymbol{p},t) = \sum_i \chi^*_\Gamma(S_i) \sum_{\boldsymbol{x}} e^{i\boldsymbol{p}\boldsymbol{x}}\, \bar{q}(\boldsymbol{x},t) q(\boldsymbol{x},t) = \left(\sum_i \chi^*_\Gamma(S_i)\right) O(\boldsymbol{p},t)\,. \tag{103}$$

Consequently, the operator $O(\boldsymbol{p},t)$ transforms according to the trivial representation A_1, for which $\sum_i \chi^*_\Gamma(S_i) \neq 0$.

In the case of equal masses, the number of irreducible representations is doubled, $\Gamma \to \Gamma^\pm$, and the momentum $\boldsymbol{p}$ is left invariant by the elements of the little group up to a sign,

$S_i\,\boldsymbol{p} = \pm\boldsymbol{p}$. Accordingly, the operators O^Γ should be symmetrized, or antisymmetrized, with respect to $\boldsymbol{p} \leftrightarrow -\boldsymbol{p}$. However, we may still work with the same operators as for unequal masses. The advantage of these operators is that they have definite momentum $\boldsymbol{p}$. The additional symmetry present in the case of equal masses has solely the effect that even angular momenta do not mix with odd angular momenta in the spectrum of the lattice Hamiltonian.

2. The case $\boldsymbol{d} = (0,0,1)$ – vector mesons

Starting from the operator

$$V(\boldsymbol{p},t) = \begin{pmatrix} V_1(\boldsymbol{p},t) \\ V_2(\boldsymbol{p},t) \\ V_3(\boldsymbol{p},t) \end{pmatrix} \qquad V_i(\boldsymbol{p},t) = \sum_{\boldsymbol{x}} e^{i\boldsymbol{p}\boldsymbol{x}}\,\bar{q}(\boldsymbol{x},t)\,\gamma_i\,q(\boldsymbol{x},t)\,, \tag{104}$$

it can easily be checked that in the case of unequal masses the operator

$$V^E(\boldsymbol{p},t) = \sum_{\boldsymbol{x}} e^{i\boldsymbol{p}\boldsymbol{x}} \begin{pmatrix} V_1(\boldsymbol{x},t) \\ V_2(\boldsymbol{x},t) \\ 0 \end{pmatrix} \tag{105}$$

transforms according to the irreducible representation E. In fact, one may use any linear combination of V_1 and V_2 to project onto E. In contrast, the third component, V_3, transforms according to the irreducible representation A_1,

$$V^{A_1}(\boldsymbol{p},t) = \sum_{\boldsymbol{x}} e^{i\boldsymbol{p}\boldsymbol{x}}\,V_3(\boldsymbol{x},t)\,. \tag{106}$$

3. The case $\boldsymbol{d} = (1,1,1)$ – vector mesons

We start again from the operator (104). Instead of (105), we now get

$$V^E(\boldsymbol{p},t) = \sum_{\boldsymbol{x}} e^{i\boldsymbol{p}\boldsymbol{x}} \begin{pmatrix} 2V_1(\boldsymbol{x},t) - V_2(\boldsymbol{x},t) - V_3(\boldsymbol{x},t) \\ 2V_2(\boldsymbol{x},t) - V_3(\boldsymbol{x},t) - V_1(\boldsymbol{x},t) \\ 2V_3(\boldsymbol{x},t) - V_1(\boldsymbol{x},t) - V_2(\boldsymbol{x},t) \end{pmatrix}\,. \tag{107}$$

The components of V^E are cyclic permutations, $\{i,j,k\} = \{1,2,3\}$, of the operator $2V_i - V_j - V_k$. Note that only two of the components of V^E are independent, in accord with the representation E being two-dimensional.

The operator projected onto the prepresentation A_1 is given by

$$V^{A_1}(\boldsymbol{p},t) = \sum_{\boldsymbol{x}} e^{i\boldsymbol{p}\boldsymbol{x}} \left(V_1(\boldsymbol{x},t) + V_2(\boldsymbol{x},t) + V_3(\boldsymbol{x},t)\right). \tag{108}$$

4. The case $\boldsymbol{d} = (0,0,1)$ *– Δ resonance*

We start from the interpolating operator of the Δ^+ resonance,

$$\Delta^+_\alpha(\boldsymbol{p},t) = \begin{pmatrix} \Delta^+_{1\alpha}(\boldsymbol{p},t) \\ \Delta^+_{2\alpha}(\boldsymbol{p},t) \\ \Delta^+_{3\alpha}(\boldsymbol{p},t) \end{pmatrix} \tag{109}$$

with, for example,

$$\begin{aligned} \Delta^+_{i\alpha}(\boldsymbol{p},t) &= \sum_{\boldsymbol{x}} e^{i\boldsymbol{p}\boldsymbol{x}} \left\{2(u^T(\boldsymbol{x},t)C\gamma_i d(\boldsymbol{x},t)u_\alpha(\boldsymbol{x},t) + (u^T(\boldsymbol{x},t)C\gamma_i u(\boldsymbol{x},t)d_\alpha(\boldsymbol{x},t)\right\} \\ &= \sum_{\boldsymbol{x}} e^{i\boldsymbol{p}\boldsymbol{x}} \Delta^+_{i\alpha}(\boldsymbol{x},t)\,. \end{aligned} \tag{110}$$

Under space rotations the operator $\Delta^+_{i\alpha}(\boldsymbol{p},t)$ transforms as

$$(\hat{R}\Delta)^+_{i\alpha}(\boldsymbol{x},t) = S_{\alpha\beta}(R)\, A_{ij}(R)\, \Delta^+_{j\beta}(R^{-1}\boldsymbol{x},t)\,, \quad S(R) = \begin{pmatrix} \check{S}(R) & 0 \\ 0 & \check{S}(R) \end{pmatrix}, \tag{111}$$

where $A(R)$ and $\check{S}(R)$ are 3×3 and 2×2 irreducible matrix representations of $SU(2)$, respectively. Under space inversions the operator transforms as

$$(\hat{I}\Delta)^+_{i\alpha}(\boldsymbol{x},t) = (\gamma_0)_{\alpha\beta}\Delta^+_{i\beta}(-\boldsymbol{x},t)\,. \tag{112}$$

Applying (99), the operators projected onto the irreducible representations G_1 and G_2 turn out to be

$$\Delta^{+G_1}_\alpha = \sum_{\boldsymbol{x}} e^{i\boldsymbol{p}\boldsymbol{x}} \begin{pmatrix} \Delta^+_{1\alpha}(\boldsymbol{x},t) + i(\Sigma_3)_{\alpha\beta}\Delta^+_{2\beta}(\boldsymbol{x},t) \\ \Delta^+_{2\alpha}(\boldsymbol{x},t) - i(\Sigma_3)_{\alpha\beta}\Delta^+_{1\beta}(\boldsymbol{x},t) \\ 2\Delta^+_{3\alpha}(\boldsymbol{x},t) \end{pmatrix} \tag{113}$$

and

$$\Delta^{+G_2}_\alpha = \sum_{\boldsymbol{x}} e^{i\boldsymbol{p}\boldsymbol{x}} \begin{pmatrix} \Delta^+_{1\alpha}(\boldsymbol{x},t) - i(\Sigma_3)_{\alpha\beta}\Delta^+_{2\beta}(\boldsymbol{x},t) \\ \Delta^+_{2\alpha}(\boldsymbol{x},t) + i(\Sigma_3)_{\alpha\beta}\Delta^+_{1\beta}(\boldsymbol{x},t) \\ 0 \end{pmatrix}, \tag{114}$$

respectively, where

$$\Sigma_3 = \begin{pmatrix} \sigma_3 & 0 \\ 0 & \sigma_3 \end{pmatrix} . \tag{115}$$

B. Two-particle operators

1. *The case* $\boldsymbol{d} = (0,0,1)$ – *product of two (pseudo-)scalar fields*

We start from the operator

$$O(\boldsymbol{p},\boldsymbol{q},t) = \sum_{\boldsymbol{x},\boldsymbol{y}} e^{i(\boldsymbol{p}\boldsymbol{x}+\boldsymbol{q}(\boldsymbol{x}-\boldsymbol{y}))}\phi_1(\boldsymbol{x},t)\,\phi_2(\boldsymbol{y},t)\,. \tag{116}$$

In the case of unequal masses the operator that transforms according to the irreducible representation Γ is given by

$$O^{\Gamma}(\boldsymbol{p},\boldsymbol{q},t) = \sum_{i=1}^{8} \chi^*_{\Gamma}(S_i) \sum_{\boldsymbol{x},\boldsymbol{y}} e^{i(\boldsymbol{p}\boldsymbol{x}+(S_i\boldsymbol{q})(\boldsymbol{x}-\boldsymbol{y}))}\phi_1(\boldsymbol{x},t)\,\phi_2(\boldsymbol{y},t)\,, \tag{117}$$

where

i	$S_i\boldsymbol{q}$
1	(q_1,q_2,q_3)
2	$(q_2,-q_1,q_3)$
3	$(-q_2,q_1,q_3)$
4	$(-q_1,-q_2,q_3)$
5	$(-q_2,-q_1,q_3)$
6	(q_2,q_1,q_3)
7	$(-q_1,q_2,q_3)$
8	$(q_1,-q_2,q_3)$

(118)

From this expression one readily obtains, for example, the operator that transforms according to the representation E,

$$O^{E}(\boldsymbol{p},\boldsymbol{q},t) = \sum_{\boldsymbol{x},\boldsymbol{y}} e^{i\boldsymbol{p}\boldsymbol{x}} \left(e^{i\boldsymbol{q}_\perp(\boldsymbol{x}-\boldsymbol{y})_\perp} - e^{-i\boldsymbol{q}_\perp(\boldsymbol{x}-\boldsymbol{y})_\perp}\right) e^{i\boldsymbol{q}_\parallel(\boldsymbol{x}-\boldsymbol{y})_\parallel}\,\phi_1(\boldsymbol{x},t)\,\phi_2(\boldsymbol{y},t)\,, \tag{119}$$

where $\boldsymbol{q}_\parallel = (0,0,q_3)$ and $\boldsymbol{q}_\perp = (q_1,q_2,0)$, and similarly for $\boldsymbol{x}$, $\boldsymbol{y}$.

2. The case $\boldsymbol{d} = (1,1,0)$ – product of pion and nucleon fields

This case is trivial, as only the irreducible representation G_1 contributes. Any operator, for example

$$O(\boldsymbol{p},\boldsymbol{q},t) = \sum_{\boldsymbol{x},\boldsymbol{y}} e^{i(\boldsymbol{p}\boldsymbol{x}+\boldsymbol{q}(\boldsymbol{x}-\boldsymbol{y}))}\, \pi(\boldsymbol{x},t)\, N(\boldsymbol{y},t)\,, \tag{120}$$

will transform according to G_1.

Having the characters $\chi(\Gamma)$ of the irreducible representations Γ of the little groups at hand, it should be no problem to construct operators that transform according to any other representation. Examples of meson-baryon operators projected onto representations G_2 in the case of $\boldsymbol{d} = (0,0,1)$ and B_1, B_2 in the case of $\boldsymbol{d} = (1,1,1)$ will be given in a separate publication [18], together with numerical results.

VIII. CONCLUSIONS

In this work we have extended previous work by Lüscher [1] and others [2, 6–8] on determining the scattering phases from the energy levels of the (lattice) Hamiltonian in a finite volume to meson and baryon resonances of arbitrary masses and arbitrary total momenta $\boldsymbol{P} = (2\pi n/L)\,(d_1,d_2,d_3)$ with $d_i = 0,\pm 1$, $n \in \mathbb{Z}$. Explicit formulae for the phase shifts have been given for meson resonances with angular momentum $l \leq 2$ and for baryon resonances with spin $J \leq 3/2$ and orbital angular momentum $l \leq 2$. That covers essentially all elastic two-body resonances. There are several advantages to performing simulations with nonvanishing total momenta. This includes making the avoided level crossing in P-wave decays occur at a smaller volume, in the case the scattering particles have different mass, and making a wider set of energy levels available on a single lattice volume.

The drawback is that the individual partial waves will mix in general. Neglecting D waves, this is the case for all S-wave meson resonances and all S- and P-wave spin-1/2 baryon resonances. To compute the P-wave phase shift $\delta_{\frac{1}{2}1}$, for example, one will need input from $\delta_{\frac{1}{2}0}$. One might be lucky though and find the latter to be small, because no low-lying positive parity S-wave spin-1/2 pion-nucleon resonance has been reported [13]. This is one of the mysteries of baryon spectroscopy.

The success of the method depends on our ability to construct operators that will transform according to the desired representation of the little group. We have outlined the

general procedure of how to construct such operators from the character tables, and given a few explicit examples of single-particle and two-particle operators.

Acknowledgment

We like to thank Sasa Prelovsek for discussions. This work has been supported in part by the EU Integrated Infrastructure Initiative *HadronPhysics3* under Grant Agreement no. 283286 and by the DFG under contract SFB/TR 55 (Hadron Physics from Lattice QCD) and SFB/TR 16 (Subnuclear Structure of Matter), as well as by COSY FFE under contract no. 41821485 (COSY 106). AR acknowledges support of the Shota Rustaveli Science Foundation (Project DI/13/02).

Appendix A: Zeta functions

A valid representation of the zeta function for $\delta = 1$ is given by [10]

$$Z_{lm}^{\boldsymbol{\Delta}}(1,q^2) = \sum_{\substack{\boldsymbol{z}\in P_{\boldsymbol{\Delta}} \\ |\boldsymbol{z}|<\lambda}} \frac{\mathcal{Y}_{lm}(\boldsymbol{z})}{\boldsymbol{z}^2-q^2} + (2\pi)^3 \int_0^\infty dt \, \left[e^{tq^2} \, K_{lm}^{\boldsymbol{\Delta}\,\lambda}(t,\boldsymbol{0}) - \frac{\gamma\,\delta_{l0}\,\delta_{m0}}{(4\pi)^2 t^{3/2}} \right] , \tag{A1}$$

where

$$K_{lm}^{\boldsymbol{\Delta}\,\lambda}(t,\boldsymbol{r}) = K_{lm}^{\boldsymbol{\Delta}}(t,\boldsymbol{r}) - \frac{1}{(2\pi)^3} \sum_{\substack{\boldsymbol{z}\in P_{\boldsymbol{\Delta}} \\ |\boldsymbol{z}|<\lambda}} \mathcal{Y}_{lm}(\boldsymbol{z})\, e^{i\boldsymbol{z}\boldsymbol{r}-t\boldsymbol{z}^2} \tag{A2}$$

and $K_{lm}^{\boldsymbol{\Delta}}(t,\boldsymbol{r})$ is the heat kernel of the Laplace operator on the $\boldsymbol{\Delta}$-periodic lattice,

$$K_{lm}^{\boldsymbol{\Delta}}(t,\boldsymbol{r}) = \frac{1}{(2\pi)^3} \sum_{\boldsymbol{z}\in P_{\boldsymbol{\Delta}}} \mathcal{Y}_{lm}(\boldsymbol{z})\, e^{i\boldsymbol{z}\boldsymbol{r}-t\boldsymbol{z}^2} \, . \tag{A3}$$

This leads to

$$\begin{aligned} Z_{lm}^{\boldsymbol{\Delta}}(1,q^2) = & \sum_{\substack{\boldsymbol{z}\in P_{\boldsymbol{\Delta}} \\ |\boldsymbol{z}|<\lambda}} \frac{\mathcal{Y}_{lm}(\boldsymbol{z})}{\boldsymbol{z}^2-q^2}\, e^{-(\boldsymbol{z}^2-q^2)} + \int_1^\infty dt \sum_{\substack{\boldsymbol{z}\in P_{\boldsymbol{\Delta}} \\ |\boldsymbol{z}|>\lambda}} \mathcal{Y}_{lm}(\boldsymbol{z})\, e^{-t(\boldsymbol{z}^2-q^2)} \\ & + \int_0^1 dt \, \left[\sum_{\boldsymbol{z}\in P_{\boldsymbol{\Delta}}} \mathcal{Y}_{lm}(\boldsymbol{z})\, e^{-t(\boldsymbol{z}^2-q^2)} - \gamma\,\frac{\pi}{2}\,\delta_{l0}\,\delta_{m0}\,\frac{1}{t^{3/2}} \right] - \gamma\,\frac{\pi}{4}\,\delta_{l0}\,\delta_{m0} \end{aligned} \tag{A4}$$

with both integrals being well defined for a suitable choice of λ. Indeed, using the relation

$$\sum_{\boldsymbol{z}\in P_{\boldsymbol{\Delta}}} \mathcal{Y}_{lm}(\boldsymbol{z})\, e^{-t\boldsymbol{z}^2} = \gamma \left(\frac{\pi}{t}\right)^{3/2} \left(\frac{i}{2t}\right)^l \sum_{\boldsymbol{n}\in\mathbb{Z}^3} e^{-i\pi\boldsymbol{n}\boldsymbol{\Delta}} \mathcal{Y}_{lm}(2\pi\boldsymbol{\gamma}\boldsymbol{n})\, e^{-(2\pi\boldsymbol{\gamma}\boldsymbol{n})^2/4t} \, , \tag{A5}$$

the sum over $\boldsymbol{z}\in P_{\boldsymbol{\Delta}}$ in the second integral can be expressed in terms of a sum over $\boldsymbol{n}\in\mathbb{Z}^3$, which finally gives

$$\begin{aligned} Z_{lm}^{\boldsymbol{\Delta}}(1,q^2) = & \sum_{\boldsymbol{z}\in P_{\boldsymbol{\Delta}}} \frac{\mathcal{Y}_{lm}(\boldsymbol{z})}{\boldsymbol{z}^2-q^2}\, e^{-(\boldsymbol{z}^2-q^2)} + \gamma\,\frac{\pi}{2}\,\delta_{l0}\,\delta_{m0}\,F(q) \\ & + \gamma\pi^{3/2} \int_0^1 dt\, \frac{e^{tq^2}}{t^{3/2}} \left(\frac{i}{2t}\right)^l \sum_{\substack{\boldsymbol{n}\in\mathbb{Z}^3 \\ \boldsymbol{n}\neq 0}} e^{-i\pi\boldsymbol{n}\boldsymbol{\Delta}}\, \mathcal{Y}_{lm}(2\pi\boldsymbol{\gamma}\boldsymbol{n})\, e^{-(\pi\boldsymbol{\gamma}\boldsymbol{n})^2/t} \, , \end{aligned} \tag{A6}$$

where

$$F(q) = \int_0^1 dt \frac{e^{tq^2}-1}{t^{3/2}} - 2 = \sum_{n=0}^\infty \frac{q^{2n}}{(n-1/2)\,n!} \, . \tag{A7}$$

---

[1] M. Lüscher, Commun. Math. Phys. **105** (1986) 153; Nucl. Phys. B **364**, 237 (1991).

[2] K. Rummukainen and S. A. Gottlieb, Nucl. Phys. B **450**, 397 (1995) [hep-lat/9503028].

[3] W. Bietenholz, V. Bornyakov, M. Göckeler, R. Horsley, W.G. Lockhart, Y. Nakamura, H. Perlt, D. Pleiter, P.E.L. Rakow, G. Schierholz, A. Schiller, T. Streuer, H. Stüben, F. Winter, J.M. Zanotti [QCDSF Collaboration], Phys. Rev. D **84**, 054509 (2011) [arXiv:1102.5300 [hep-lat]].

[4] S. Dürr, Z. Fodor, J. Frison, C. Hoelbling, R. Hoffmann, S.D. Katz, S. Krieg, T. Kurth, L. Lellouch, T. Lippert, K.K. Szabo, G. Vulvert [BMW Collaboration], Science **322**, 1224 (2008) [arXiv:0906.3599 [hep-lat]].

[5] Z. Davoudi and M. J. Savage, Phys. Rev. D **84**, 114502 (2011) [arXiv:1108.5371 [hep-lat]].

[6] Z. Fu, Phys. Rev. D **85**, 014506 (2012) [arXiv:1110.0319 [hep-lat]].

[7] X. Feng, K. Jansen, D.B. Renner [ETM Collaboration], PoS LAT **2010**, 104 (2010) [arXiv:1104.0058 [hep-lat]].

[8] L. Leskovec and S. Prelovsek, arXiv:1202.2145 [hep-lat].

[9] M. Döring, U.-G. Meißner, E. Oset, A. Rusetsky, arXiv:1205.4838 [hep-lat].

[10] M. Lüscher, Nucl. Phys. B **354**, 531 (1991).

[11] A. Messiah, "Quantum Mechanics, Volume II", Dover Publications (2000).

[12] V. Bernard, M. Lage, U.-G. Meißner, A. Rusetsky, JHEP **0808** (2008) 024 [arXiv:0806.4495 [hep-lat]].

[13] K. Nakamura *et al.* [Particle Data Group], J. Phys. G **37**, 075021 (2010).

[14] C. E. Thomas, R. G. Edwards and J. J. Dudek, Phys. Rev. D **85**, 014507 (2012) [arXiv:1107.1930 [hep-lat]].

[15] J. J. Dudek, R. G. Edwards and C. E. Thomas, arXiv:1203.6041 [hep-ph].

[16] J. Foley, J. Bulava, Y. -C. Jhang, K. J. Juge, D. Lenkner, C. Morningstar and C. H. Wong, arXiv:1205.4223 [hep-lat].

[17] J. P. Elliott and P. G. Dawber, "Symmetry in Physics, Volume I: Principles And Simple Applications", Macmillan (1979).

[18] M. Göckeler, R. Horsley, M. Lage, U.-G. Meißner, R. Millo, A. Nogga, P.E.L. Rakow, A. Rusetsky, G. Schierholz, J. Zanotti, work in progress.